

AD-A205 256

NAVAL POSTGRADUATE SCHOOL Monterey, California



THESIS

TARGET VOLTAGE RESPONSE IN REACTION TO
LASER RADIATION

by

Richard M. Harkins

December 1988

Thesis Advisor

Fred R. Schwirzke

Approved for public release; distribution is unlimited.

DTIC
ELECTE
MAR 14 1989
S H D

88 88 88 1 2 3 4 5

Unclassified

security classification of this page

ADA205256

REPORT DOCUMENTATION PAGE

1a Report Security Classification Unclassified		1b Restrictive Markings	
2a Security Classification Authority		3 Distribution Availability of Report	
2b Declassification Downgrading Schedule		Approved for public release; distribution is unlimited.	
4 Performing Organization Report Number(s)		5 Monitoring Organization Report Number(s)	
6a Name of Performing Organization Naval Postgraduate School	6b Office Symbol (if applicable) 61	7a Name of Monitoring Organization Naval Postgraduate School	
6c Address (city, state, and ZIP code) Monterey, CA 93943-5000		7b Address (city, state, and ZIP code) Monterey, CA 93943-5000	
8a Name of Funding Sponsoring Organization	8b Office Symbol (if applicable)	9 Procurement Instrument Identification Number	
8c Address (city, state, and ZIP code)		10 Source of Funding Numbers	
		Program Element No	Project No
		Task No	Work Unit Accession No
11 Title (include security classification) TARGET VOLTAGE RESPONSE IN REACTION TO LASER RADIATION			
12 Personal Author(s) Richard M. Harkins			
13a Type of Report Master's Thesis	13b Time Covered From To	14 Date of Report (year, month, day) December 1988	15 Page Count 74
16 Supplementary Notation The views expressed in this thesis are those of the author and do not reflect the official policy or position of the Department of Defense or the U.S. Government.			
17 Cosati Codes		18 Subject Terms (continue on reverse if necessary and identify by block number)	
Field	Group	Subgroup	laser target damage; aluminum target voltage fluctuation.
19 Abstract (continue on reverse if necessary and identify by block number)			
A five microsecond, 15 joule, pulsed CO ₂ Laser was used to irradiate polished 2024 aluminum targets. The target voltage response (TVR) was measured with respect to the incident laser radiation and showed a pulse width on the order of 30 nanoseconds. The voltage was measured at values from 22 to 140 volts with resistances varying from one ohm to two mega-ohms. The TVR was correlated to the emission and blow-off of electrons from the target surface and the possible ignition of a Laser Supported Detonation wave. The TVR, laser pulse, and flash associated with target surface breakdown were time correlated and shown to happen within the first 170 nanoseconds of the five microsecond laser pulse. Currents up to 500 amps were observed when the resistance to ground was reduced to less than 1 ohm. Also, the magnitude of the TVR was shown to be a function of background gas pressure. <i>See notes</i>			
20 Distribution Availability of Abstract <input checked="" type="checkbox"/> unclassified unlimited <input type="checkbox"/> same as report <input type="checkbox"/> DTIC users		21 Abstract Security Classification Unclassified	
22a Name of Responsible Individual Fred R. Schwirzke		22b Telephone (include Area code) (408) 646-2635	22c Office Symbol 61sw

DD FORM 1473, 84 MAR

83 APR edition may be used until exhausted
All other editions are obsolete

security classification of this page

Unclassified

Approved for public release; distribution is unlimited.

Target Voltage Response in Reaction to Laser Radiation

by

Richard M. Harkins
Lieutenant, United States Navy
B.S., United States Naval Academy, 1981

Submitted in partial fulfillment of the
requirements for the degree of

MASTER OF SCIENCE IN PHYSICS

from the

NAVAL POSTGRADUATE SCHOOL
December 1988

Author:

Richard M Harkins

Richard M. Harkins

Approved by:

Fred R. Schwirzke

Fred R. Schwirzke, Thesis Advisor

Alfred W. M. Cooper

Alfred W. M. Cooper, Second Reader

Karlheinz E. Woehler

Karlheinz E. Woehler, Chairman,
Department of Physics

Gordon E. Schacher

Gordon E. Schacher,
Dean of Science and Engineering

ABSTRACT

A five microsecond, 15 joule, pulsed CO₂ Laser was used to irradiate polished 2024 aluminum targets. The target voltage response (TVR) was measured with respect to the incident laser radiation and showed a pulse width on the order of 30 nanoseconds. The voltage was measured at values from 22 to 140 volts with resistances varying from one ohm to two mega-ohms. The TVR was correlated to the emission and blow-off of electrons from the target surface and the possible ignition of a Laser Supported Detonation wave. The TVR, laser pulse, and flash associated with target surface breakdown were time correlated and shown to happen within the first 170 nanoseconds of the five microsecond laser pulse. Currents up to 500 amps were observed when the resistance to ground was reduced to less than 1 ohm. Also, the magnitude of the TVR was shown to be a function of background gas pressure.



Accession For	
NTIS GRA&I	<input checked="" type="checkbox"/>
DTIC TAB	<input type="checkbox"/>
Unannounced	<input type="checkbox"/>
Justification	
By _____	
Distribution/ _____	
Availability Codes	
Dist	Avail and/or Special
A-1	

TABLE OF CONTENTS

I. INTRODUCTION	1
II. BACKGROUND AND THEORY	3
A. PLASMA GROWTH	3
B. LASER SUPPORTED ABSORPTION WAVES	5
1. LSD Wave	7
2. LSC Wave	7
3. LSB Wave	7
4. Ignition and Transition of Absorption Waves	8
a. Ignition, Onset of Target Surface Breakdown	8
b. Transition to a Critical Plasma Density	9
C. UNIPOLAR-ARCING	10
1. Quasi-Neutrality	10
2. Floating Potential	11
3. Sheath Width, Debye Length	11
4. Unipolar-Arc Model	12
III. EXPERIMENTAL METHOD	17
A. OBJECTIVES	17
B. APPARATUS	17
C. PROCEDURE	17
1. Target Preparation	17
2. Voltage Measurement	17
3. Voltage, Pulse, Flash Correlation	19
4. Voltage VS Pressure Comparison	20
5. Current Calculations	20
6. Energy per Pulse	21
IV. EXPERIMENTAL RESULTS	22
A. TARGET VOLTAGE RESPONSE	22
B. TVR, PULSE, AND FLASH CORRELATION	31

1. Chop Mode	31
2. Multiple Exposures	39
C. PRESSURE DEPENDENCE OF THE TVR	44
D. CURRENT DEDUCTIONS	44
V. ANALYSIS OF DATA	50
A. DATA CHARACTERISTICS	50
B. DISCUSSION	50
1. TVR Measurement, Electron Emission	50
2. TVR, Laser Pulse, Flash correlation	53
3. Current Deductions	53
4. TVR and Pressure Dependence	54
C. CONCLUSIONS	54
APPENDIX A	56
APPENDIX B	57
APPENDIX C	58
APPENDIX D	60
A. CALCULATION OF TIME TO TVR.	60
B. CALCULATION OF LASER PULSE INTENSITY	61
C. THERMIONIC EMISSION	61
D. CALCULATION OF MEAN TVR PULSE WIDTH	62
LIST OF REFERENCES	63
INITIAL DISTRIBUTION LIST	65

LIST OF TABLES

Table 1.	TARGET VOLTAGE RESPONSE DATA	23
Table 2.	VERTICAL AND HORIZONTAL MODE SETTINGS	31
Table 3.	RAW DATA	56
Table 4.	ENERGY PER SHOT	57
Table 5.	LASER FLOW, CHARGING CURRENT SETTINGS	58
Table 6.	OSCILLOSCOPE SETTINGS FOR VOLTAGE MEASUREMENT ...	58
Table 7.	OSCILLOSCOPE SETTINGS FOR TVR CORRELATION, 3 INPUTS	59

LIST OF FIGURES

Figure 1. Wave Superposition and Plasma Growth	4
Figure 2. Laser Absorption Waves	6
Figure 3. Laser Supported Blast Wave at Oblique Incidence	7
Figure 4. Plasma Loss to the Surface	13
Figure 5. Unipolar Arc Model	14
Figure 6. Depiction of Surface Whisker and Associated Electric Field	15
Figure 7. Typical Arcing Craters	16
Figure 8. Experimental Arrangement	18
Figure 9. Circuit Diagram for Voltage Measurement	19
Figure 10. Circuit Diagram for Time Correlation	20
Figure 11. Voltage Response, Shot 1	24
Figure 12. Voltage Response, Shot 2	25
Figure 13. Voltage Response, Shot 3	26
Figure 14. Voltage Response, Shot 4	27
Figure 15. Voltage Response, Shot 5	28
Figure 16. Voltage Response, Shot 6	29
Figure 17. Voltage Response, Shot 7	30
Figure 18. TVR and Laser Pulse, Shot 1	32
Figure 19. TVR and Laser Pulse, Shot 2	33
Figure 20. TVR and Laser Pulse, Shot 3	34
Figure 21. TVR and Laser Pulse, Shot 4	35
Figure 22. TVR and Laser Pulse, Shot 5	36
Figure 23. Flash and Laser Pulse, Shot 6	37
Figure 24. Flash and TVR, Shot 7	38
Figure 25. TVR, Shot 1	40
Figure 26. Laser Pulse, Shot 2	41
Figure 27. Flash, Shot 3	42
Figure 28. TVR, Laser Pulse, Flash, Shot 4	43
Figure 29. Voltage vs Pressure Relationship	44
Figure 30. Current vs Resistance, Log Scale	46
Figure 31. Current vs Resistance, Two Mega-Ohms to 110 Ohms	47

Figure 32. Current vs Resistance, 36 to 15 Ohms	48
Figure 33. Current vs Resistance, 1 to 0.1 Ohms	49
Figure 34. Characteristics of the TVR	52
Figure 35. Laser Pulse Extrapolation	60

I. INTRODUCTION

When a laser pulse interacts with a target, several phenomena occur which result in damage to the target surface. These include a variety of thermal, impulse and electrical effects. It has been established by research conducted at the Naval Postgraduate School that when laser-target coupling creates a plasma, the electrical effect (Unipolar-Arcing)¹ is the primary damage mechanism [ref. 1]. The theory of the Unipolar-Arc was first discussed by Robson and Thonemann in 1958 [ref. 2]. Their research, in part, focused on plasma surface interactions and the arc sustained therein. Subsequently, Schwirzke has refined the Unipolar-Arc model by elaborating on the set-up of electric fields in the plasma which drive the arc [Ref. 1].

Further investigations of this model have suggested that large currents may be induced within a target subsequent to plasma growth.² Specifically, an experiment conducted in Garching, Germany in 1983 showed that laser irradiances of 3.33×10^{11} watts incident on spherical metal targets caused enormous plasma growth and damage. In fact, a plasma literally exploded from the copper stalk on which the targets were mounted [ref. 3]. Accepted theory indicates that in order to create a plasma, an initial electron density of sufficient temperature must be present in order to create ions from surrounding neutrals, via collisions. However, where these initial electrons come from is little understood. In fact, understanding of the first events in the laser-target interaction is significantly lacking. Nevertheless, it was postulated that if the target were the source of the initial electron density, then to sustain any emission of electrons from the target surface, a current would have to exist. Therefore, it was proposed that a measurement of a target voltage response (TVR), would allow for the deduction of target currents, given that the resistance to ground was known.

The initial objective of this thesis, therefore, was to set up an experiment that would measure a TVR from which target currents could be deduced. In so doing, this would confirm and quantify the existence of target currents and show that the target was indeed the source of the initial electron density.

¹ It should be noted that Unipolar-Arcing damage occurs in both conducting and non-conducting materials.

² An application of a large current surge would be possible damage to internal electrical components.

Preliminary results showed that a TVR, of positive polarity, did occur and that its duration was on the order of 30 nanoseconds. Time correlation of the TVR with the laser pulse width showed that the event occurred very early in the laser-target interaction. The characteristics of these results indicated that what was being observed was related to the phenomenon of the Laser Supported Detonation (LSD) wave.³ This is because the emission of electrons from the target surface, which the TVR indicated, could be interpreted to be the ignition mechanism for an LSD wave. Interestingly enough, ignition mechanisms for LSD waves are poorly understood. Since 1971, at least ten have been proposed, and of these, electron emission is considered the most probable [ref. 4]. Similarly, it was determined that the laser pulse intensity was high enough to produce LSD waves based on thresholds established by Walters in the early 1970's [ref. 5]. Therefore, not only did the experiment suggest that the target was the source of the initial electron density, it also appeared that the ignition mechanism for LSD waves was electron emission. Hence, a second objective materialized from the first, which was to explain how electrons could escape from the target surface with enough energy to start ionization processes and plasma growth. In short, a model was produced explaining how the electron blow-off phenomenon occurred. Finally, the data indicated that the TVR was a function of background gas pressure.

³ An LSD wave is a type of Laser Supported Absorption wave. See Background and Theory for details.

II. BACKGROUND AND THEORY

When an intense laser pulse strikes a target, a variety of thermal, mechanical, and electrical events occur which cause the formation of a plasma and subsequent damage due to Unipolar-Arcing. The thermal effect is the vaporization process created by induced high temperatures. Mechanical effects include sputtering, impulse and shock phenomena. The electrical effect has been determined to be primarily Unipolar-Arcing [ref. 1]. In association with these, it has been shown that for laser intensities on the order of $10^7 \sim 10^8$ watts per square centimeter, a Laser Supported Detonation wave will occur. To complicate matters, none of these phenomena are unrelated. However, for clarity, the topics presented here will be dealt with as separate entities. Any significant overlap will be mentioned as required. The mechanical effects will not be dealt with in any detail. However, LSD waves could be considered mechanical due to their shock nature [ref. 6]. Suffice it to say, the overall result is the creation of a plasma which grows to a critical density, eventually shielding the target surface from the remainder of the laser pulse.

A. PLASMA GROWTH

Generally speaking, the first target response with respect to incident laser radiation, is surface contaminant desorption. This event occurs within the first few nano-seconds of the laser-target interaction and results in the immediate buildup of a neutral density close to the target surface. This buildup is essential for the plasma creation process.

For a metal target, assuming perfect reflection, a standing wave will occur at the target boundary due to the superposition of the incident and reflected electromagnetic waves. Therefore, the time average spatial intensity is given by:

$$E^2 = 4E_0^2 \sin^2\left(\frac{2\pi z}{\lambda}\right). \quad (1)$$

Maxima will occur at distances equal to $\frac{\lambda}{4}$, $\frac{3\lambda}{4}$ etc. . Assuming an initial electron density, the neutrals created by desorption will first become ionized at a distance, $D = \frac{\lambda}{4}$ from the target surface, creating a plasma. This is because the electrons will be heated most at the maxima of the standing wave, causing rapid ionization of neutrals in the region. Of course, this will occur at other standing wave maxima, but on a lesser scale

due to the fall off of the neutral density farther from the target surface and a reduction of the reflected wave due to absorption. See Figure 1.

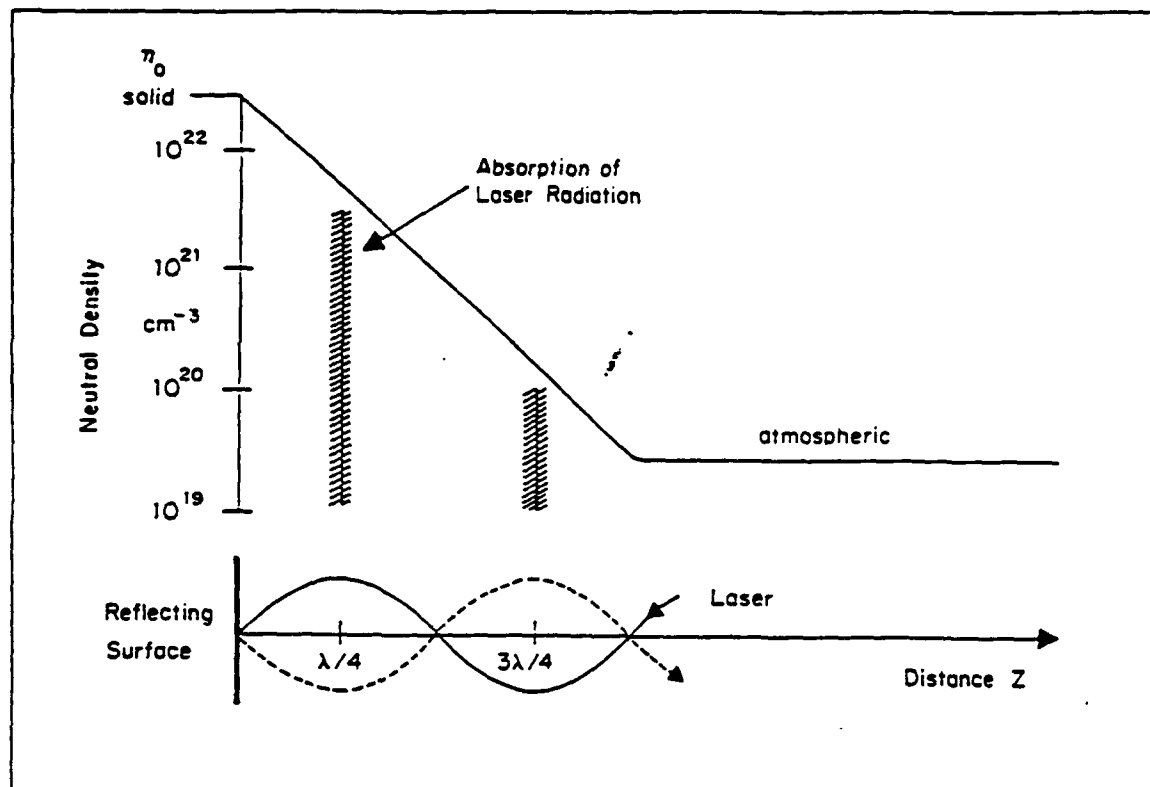


Figure 1. Wave Superposition and Plasma Growth

As this process continues, the plasma grows, eventually reaching a critical density. This occurs when the frequency of the laser (ω) equals the frequency of the plasma (ω_p). The plasma frequency is [ref. 7];

$$\omega_p = \sqrt{\frac{ne^2}{\epsilon_0 m_e}}, \quad (2)$$

where.

$\omega_p \equiv$ Plasma Frequency

$n \equiv$ Plasma Density

$m_e \equiv$ Electron Mass.

Hence, cutoff will occur at a critical density n_c when $\omega = \omega_p$,

$$n_c = \frac{m_e \epsilon_0 \omega^2}{e^2}. \quad (3)$$

This critical density is calculated to be $9.99 \times 10^{18} \text{cm}^{-3}$ for a CO_2 laser [ref. 8]. Notice that this theory is based on the assumption, that an initial electron density exists. But, how these electrons come about was not addressed. If it could be shown that the initial electrons came from the target, as could possibly occur in the ignition process for a Laser Supported Absorption (LSA) Wave, then this question would be answered.

B. LASER SUPPORTED ABSORPTION WAVES

In the early 1970's, experiments conducted at atmospheric pressure, showed that high intensity laser pulses incident on metal targets created plasmas [ref. 9]. The mechanisms by which these plasmas were formed were termed Laser Supported Absorption waves. These waves were characterized by an ignition, transition, and propagation process whereby a plasma was created and target shielding occurred. In a vacuum, desorption causes an expanding neutral gas layer from which LSA waves are able to initiate. Therefore, LSA wave theory is applicable to this experiment. LSA waves are generally grouped under three headings;

- Laser Supported Detonation (LSD) Waves
- Laser Supported Combustion (LSC) Waves
- Laser Supported Blast (LSB) Waves.

The characteristics of these waves were described by Hall et. al [ref. 9] in a report published in 1973 concerning LSA wave phenomena. The following is a summary of each wave. Refer to Figure 2 on page 6.

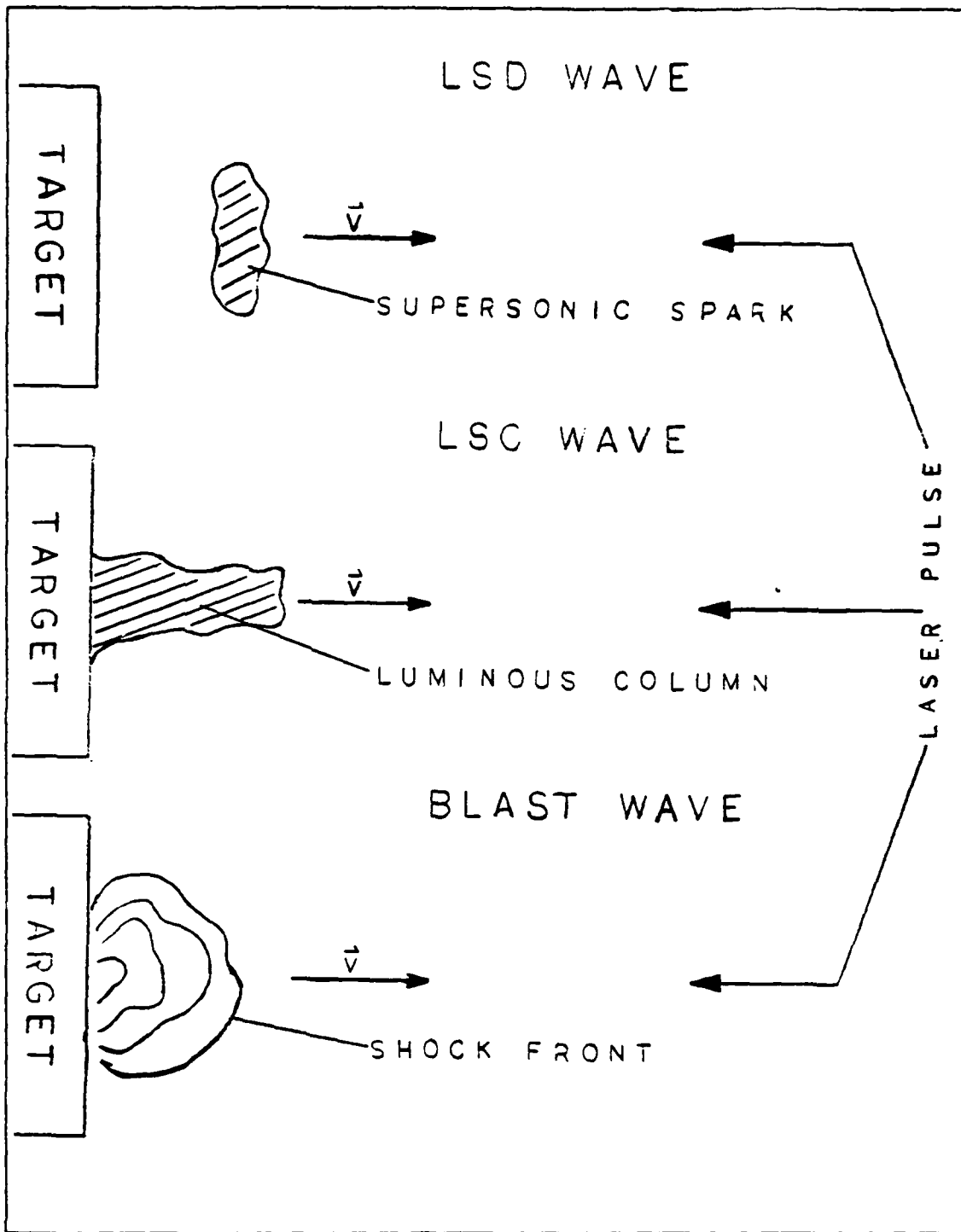


Figure 2. Laser Absorption Waves

1. LSD Wave

This wave was ignited, at atmospheric pressure, by high intensity laser radiation (approximately $10^7 \sim 10^8$ watts per square centimeter) and was characterized by what looked like a *supersonic spark* that traveled up the incident laser pulse. [ref. 4]

2. LSC Wave

The Laser Supported Combustion wave appeared as a luminous column which propagated at less than the speed of sound up the incident laser pulse while remaining in contact with the target surface. LSC wave propagation occurred when incident laser pulse intensity was on the order of $10^5 \sim 10^6$ watts per square centimeter. [ref. 4]

3. LSB Wave

Blast waves were shock fronts consisting of plasma jets that propagated outward normal to the target surface regardless of the angle of incidence of the laser pulse. Note that the LSB wave can be experimentally distinguished from the LSD or LSC wave by allowing the laser pulse to be incident upon the target at an angle other than normal. This affords discrimination between the waves because the LSC and LSD waves propagate up the incident pulse while the LSB wave propagates normal to the target surface as discussed [ref. 9]. See Figure 3.

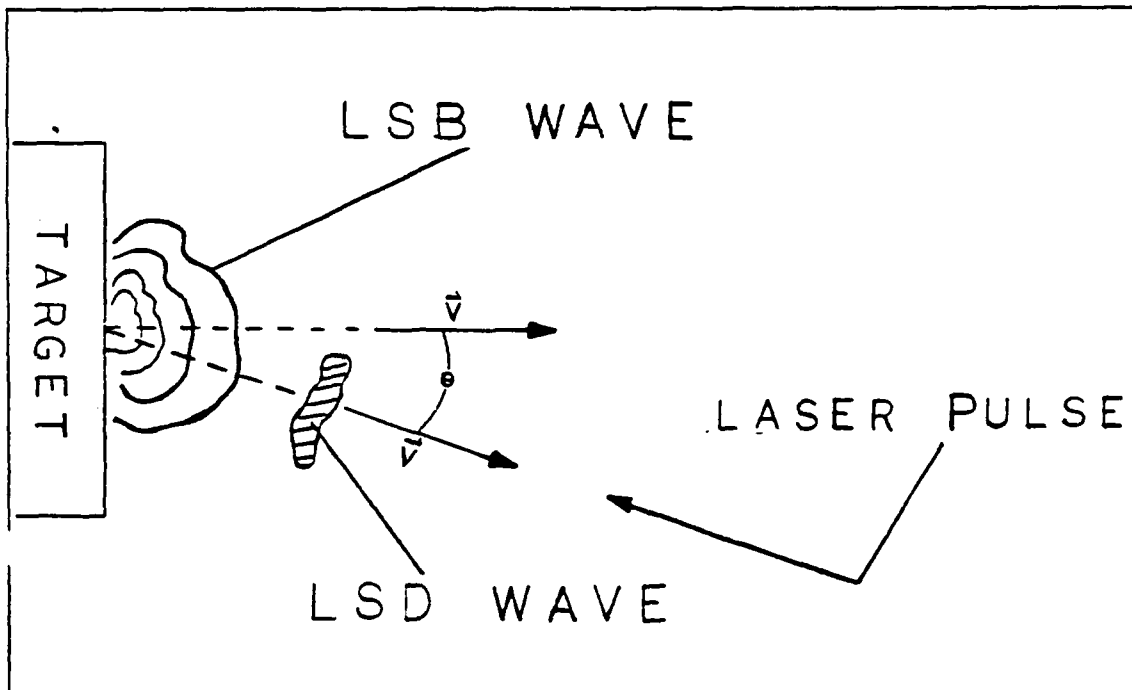


Figure 3. Laser Supported Blast Wave at oblique incidence

4. Ignition and Transition of Absorption Waves

As mentioned, the LSA wave was treated as an ignition and transition process leading to the growth of a plasma.⁴ The ignition process was where the first few electrons and ions were produced. For example, these first few electrons could come from the target surface as a consequence of the laser-target interaction. These electrons would, in turn, start the ionization process. The transition process was where initial ionization was carried into a dense plasma. Currently, the ignition process is considered the onset of target surface breakdown, while the transition process leads to the critical density.

a. Ignition, Onset of Target Surface Breakdown

Harrison and Neighbours [ref. 4] summarized in their report that the surface ignition process for LSA waves was not well understood. Of the ten mechanisms proposed since 1971, the more plausible are listed below.⁵

- Atom emission
- Ion emission
- Thermionic Electron emission
- Field enhanced emission
- Schottky emission

It should be noted that these ignition mechanisms concern emission with respect to atoms contained on the target surface. For electrons, they are considered to be a part of the target lattice structure. In other words, neutrals associated with background gas pressure, are not considered as ignition sources. Of the listed mechanisms, electron emission by a thermionic process, was considered the most probable for LSD waves. However, field enhanced emission also seemed possible. In either case, the assumption of an initial electron density in the development of the plasma growth theory [ref. 1] indirectly supported the assertion that electron emission was probable for LSD waves. This is because electron emission from the target surface could explain how an initial electron density could be established. Therefore, if it could be shown that electrons were emitted from the surface of the target in a time interval considered short with respect to the length of the laser pulse, then a sufficient amount of electrons would be present to start the plasma growth process. Single electron, atom, and ion emission are not feasible candidates for laser ignition mechanisms. This is because the photon energy of the CO_2

⁴ Propagation of the wave will not be dealt with here. See [ref. 4] for more information.

⁵ See [ref. 4] for detailed summaries of each.

laser is simply not large enough to impart enough energy to photo-emit an electron, atom, or ion.

b. Transition to a Critical Plasma Density

Upon completion of an ignition process, the initial plasma layer is formed. The transition to a dense plasma can best be understood as a series of productive and dissipative events. The productive processes must outweigh the dissipative in order to establish a critical density [ref. 4]. For the purposes of simplicity, this discussion will show single atom, single photon, and single electron interactions. To generalize, one would have to sum the interactions of each photon, electron, etc.. It is easy to appreciate that this process would be difficult.⁶

Any mechanism which increases the absolute number or density of electrons is productive, any which decreases the electron population is dissipative [ref. 4].

(1) *Production of Electrons and Ions.* Ordinarily, it would be assumed that photons from the laser pulse would couple with the growing neutral population due to desorption to produce either excited atoms or ions as follows.



where,

$h\nu \equiv$ Quantum of Energy

$A \equiv$ Atom

$A^+ \equiv$ Ion

$A^x \equiv$ Excited Atom

$e^- \equiv$ Electron.

However, this *multiphoton ionization* process is not probable for the CO_2 Laser because its photon energy is only 0.1 electron volts. Multiphoton ionization requires photon energies above 1 electron volt [ref. 4]. Consequently, the plasma growth mechanism

⁶ For another viewpoint see Schwirzke's treatment of plasma growth from the wave perspective [ref. 1].

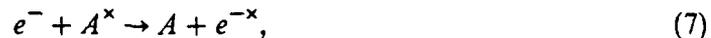
would be due to heating of free electrons. Here, sufficiently energetic electrons could ionize a neutral atom as follows;



where,

$$e^{-x} \equiv \text{Energetic Electron.}$$

(2) *Dissipation of Plasma.* The dissipative processes considered are collisional de-excitation,



radiative recombination,



and three body recombination. Three body recombination occurs when an electron collides with a third body in close proximity to an ion. The resultant transfer of momentum from the electron to the third body, allows the ion to capture the electron. It should be noted that collisional de-excitation is a dissipative event for ions but a productive event for electrons.

As the production processes overwhelm the dissipative processes the plasma density grows. When the plasma reaches a critical density, the remainder of the laser pulse is shielded from the target and the energy is transferred from the pulse to the plasma via absorption and heating. Once this hot and dense plasma is created, damage occurs to the target surface via Unipolar-Arcing.

C. UNIPOLAR-ARCING

1. Quasi-Neutrality

The dense plasma created is assumed to be *quasi-neutral*. That is;

$$n_e \approx n_i \quad (9)$$

where,

$$n_e \equiv \text{Electron Density}$$

$$n_i \equiv \text{Ion Density.}$$

In other words, the plasma is neutral enough for equation (9) to be true, but not so neutral that " ...all interesting electromagnetic forces vanish.... " [ref. 7] If some hot electrons are energetic enough to escape the boundaries of the plasma, which is normally the case, then potentials on the order of $\frac{KT_e}{e}$ would leak into the plasma causing finite electric fields to exist [ref. 7]. It is the dynamics of these electric fields which set-up and drive the arcs which cause laser pitting damage.

2. Floating Potential

A dense plasma in contact with the target means that there will be loss of electrons and ions to the target surface. Furthermore, quasi-neutrality requires that the loss rate of electrons and ions be equal. In order for this to occur, the plasma potential must always be positive with respect to the surface of the target, see Figure 4. Therefore, this sheath potential, the potential difference between the plasma and the target surface, has been defined as a floating potential and is given by,

$$V_f = \frac{KT_e}{2e} \ln\left(\frac{m_i}{2\pi m_e}\right) \quad (10)$$

where,

$KT_e \equiv$ Electron Thermal Energy

$m_i \equiv$ Ion Mass.

3. Sheath Width, Debye Length

The width of the sheath is proportional to the *Debye* length and is derived from *Poisson's* equation and the *Boltzmann* relation as follows. *Poisson's* equation is;

$$\nabla^2 \phi = - \frac{e(n_i - n_e)}{\epsilon_0} \quad (11)$$

At infinity $n_i \rightarrow n_\infty$, and the Boltzmann relation for electrons is:

$$n_e = n_\infty e^{\frac{e\phi}{KT_e}} \quad (12)$$

Expanding the exponential in a Taylor series and neglecting second order terms gives;

$$\nabla^2 \phi = - \frac{n_0 e^2}{\epsilon_0 KT_e} \quad (13)$$

where n_{∞} has been replaced by n_0 . For a planar case, $\nabla \rightarrow ik$ and $\nabla^2 \rightarrow -k^2$. Therefore,

$$-k^2\phi = -\frac{n_0 e^2 \phi}{\epsilon_0 K T_e}, \quad (14)$$

so,

$$k^2 = \frac{n_0 e^2}{\epsilon_0 K T_e}, \quad (15)$$

and if $k = \frac{1}{\lambda_d}$, then the *Debye Length* is;

$$\lambda_d^2 = \frac{K T_e \epsilon_0}{n_0 e^2}, \quad (16)$$

where,

$\epsilon_0 \equiv$ Permittivity

$n_0 \equiv$ Plasma Density.

4. Unipolar-Arc Model

The sheath potential, equation (10), controls the amount of the plasma loss to the surface. In effect, the potential accelerates ions and reflects all but the most energetic electrons such that ions and electrons reach the surface in equal numbers. See Figure 4 on page 13.

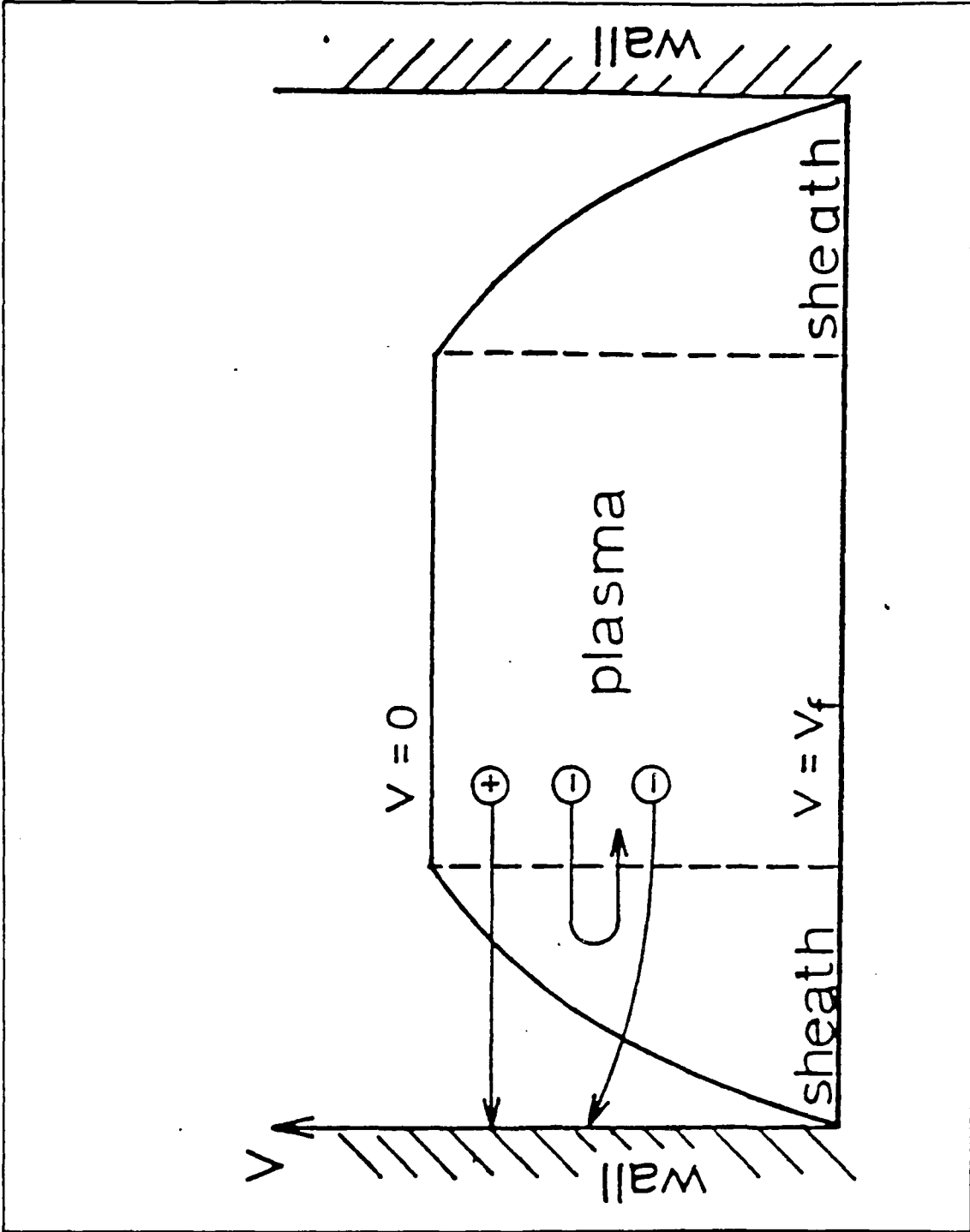


Figure 4. Plasma Loss to the Surface

Since the ions are more massive, they cause desorption and sputtering of loosely bound atoms which in turn are candidates for further ionization. Any ion or electron recombination with the surface will contribute to surface heating. The Unipolar-Arc occurs when a local increase in sheath potential due to non-uniformities of the target surface causes an increase in electric field and subsequent energetic emission of electrons from a cathode spot. Refer to Figure 5.

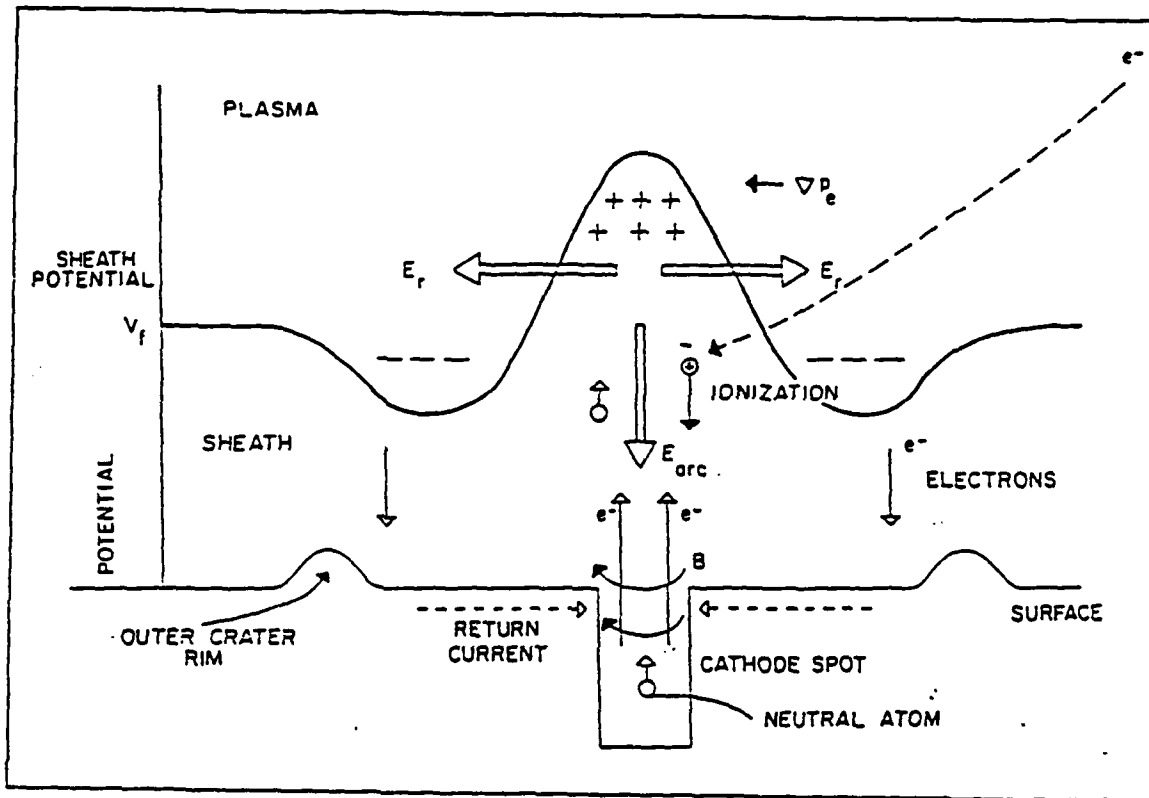


Figure 5. Unipolar Arc Model

The geometry of this potential buildup was developed by Schwirzke [ref. 1] and is depicted in Figure 5. Notice that return current is accounted for by a corresponding decrease in sheath potential adjacent to a local buildup of plasma density. Thus as electrons are emitted from the cathode, more electrons from the plasma are able to return to the surface and sustain the arc current. Therefore, the target serves as both the anode and the cathode, hence the term unipolar.

As previously mentioned, the cause of the local potential buildup was the result of non-uniformities in the target surface. Specifically, whiskers [ref. 6] can serve as cathode spots from which an arc would initiate. refer to Figure 6.

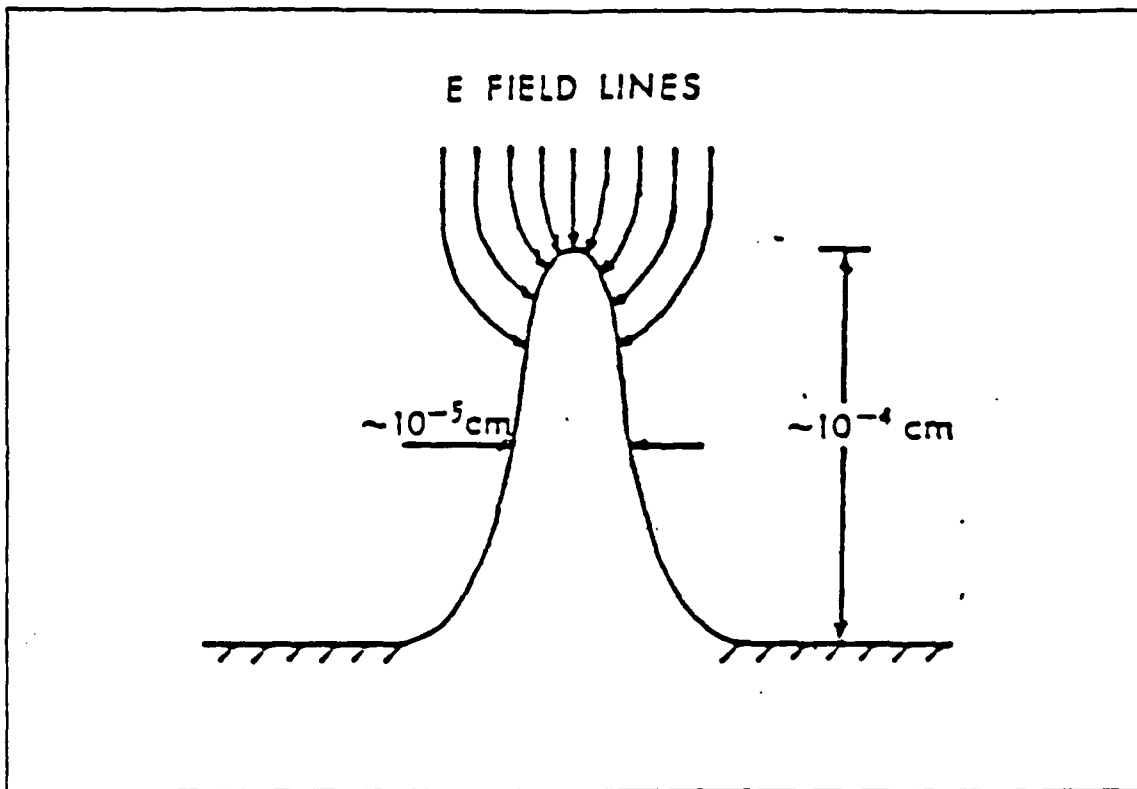


Figure 6. Depiction of Surface Whisker and Associated Electric Field

Once arcing starts, the whisker literally explodes and a crater is driven into the target surface, forming a tunnel, as high temperatures cause vaporization of surrounding atoms. Again, see Figure 5 on page 14. The arcing process will continue as long as the electron temperature and the corresponding electric field remain large enough to sustain the arc. Specifically, as the cathode spot tunnels into the surface, the surrounding plasma ends up conforming to the shape of the developing crater increasing the local plasma density. This increase of the local plasma density acts to reduce the electron temperature via collisions to a point where arcing would cease. Typical arcing craters are shown in Figure 7 on page 16.

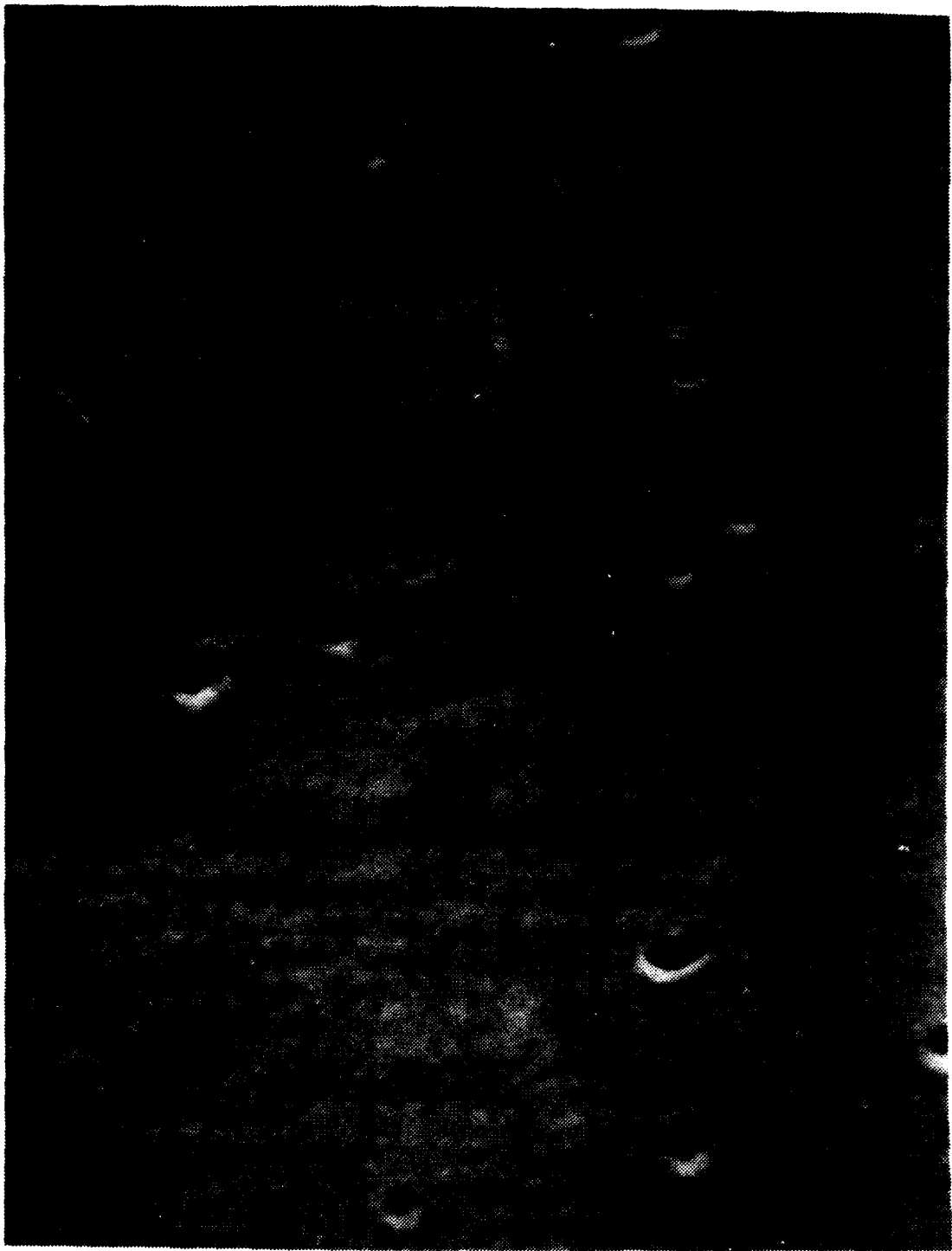


Figure 7. Typical Arcing Craters

III. EXPERIMENTAL METHOD

A. OBJECTIVES

The motivation for this experiment, as previously discussed, was to determine where the initial electron density originated, and to deduce the magnitude of target currents induced by the laser-target interaction. To this end, the following objectives were pursued.

- Measure the Target Voltage Response (TVR) of 2024 aluminum targets with respect to pulsed CO_2 laser radiation.
- Time correlate the TVR with the laser pulse and the flash associated with target surface breakdown.
- Deduce currents induced by the laser-target interaction.
- Determine background gas pressure dependence, if any, of the TVR.

B. APPARATUS

The equipment used in the experiment included the Lumonics TE-877HP CO_2 TEA pulsed laser, the VEECO vacuum system, the RJ-7000 energy meter with associated energy probe, an infrared pulse detector model DMSL-12, a photodiode flash detector, a 7104 Tektronix oscilloscope, and a Tektronix oscilloscope camera. A ZnSe beam splitter was used in conjunction with a ZnSe lens and window to direct and focus the laser pulse to the proper position on target. Wojtowich [ref. 6] gives excellent descriptions, with the exception of the photo-diode, of the mentioned apparatus and should be referenced for more information. Pertinent parameters will be provided about equipment as the context of the discussion dictates. Laser gas settings and oscilloscope set-up for each phase of the experiment are tabulated in APPENDIX C. The basic equipment arrangement was presented by Wojtowich [ref. 6] and is shown in Figure 8 on page 18.

C. PROCEDURE

1. Target Preparation

Twenty cylindrical aluminum 2024 targets were prepared from one-half inch diameter aluminum stock. The targets were machined to approximately one-half inch lengths and the surfaces were prepared by polishing with 0.05 micron alumina.

2. Voltage Measurement

In order to measure the TVR, a single 12 gage copper lead was connected to the target, axially, along its edge. The target was isolated from the vacuum chamber by

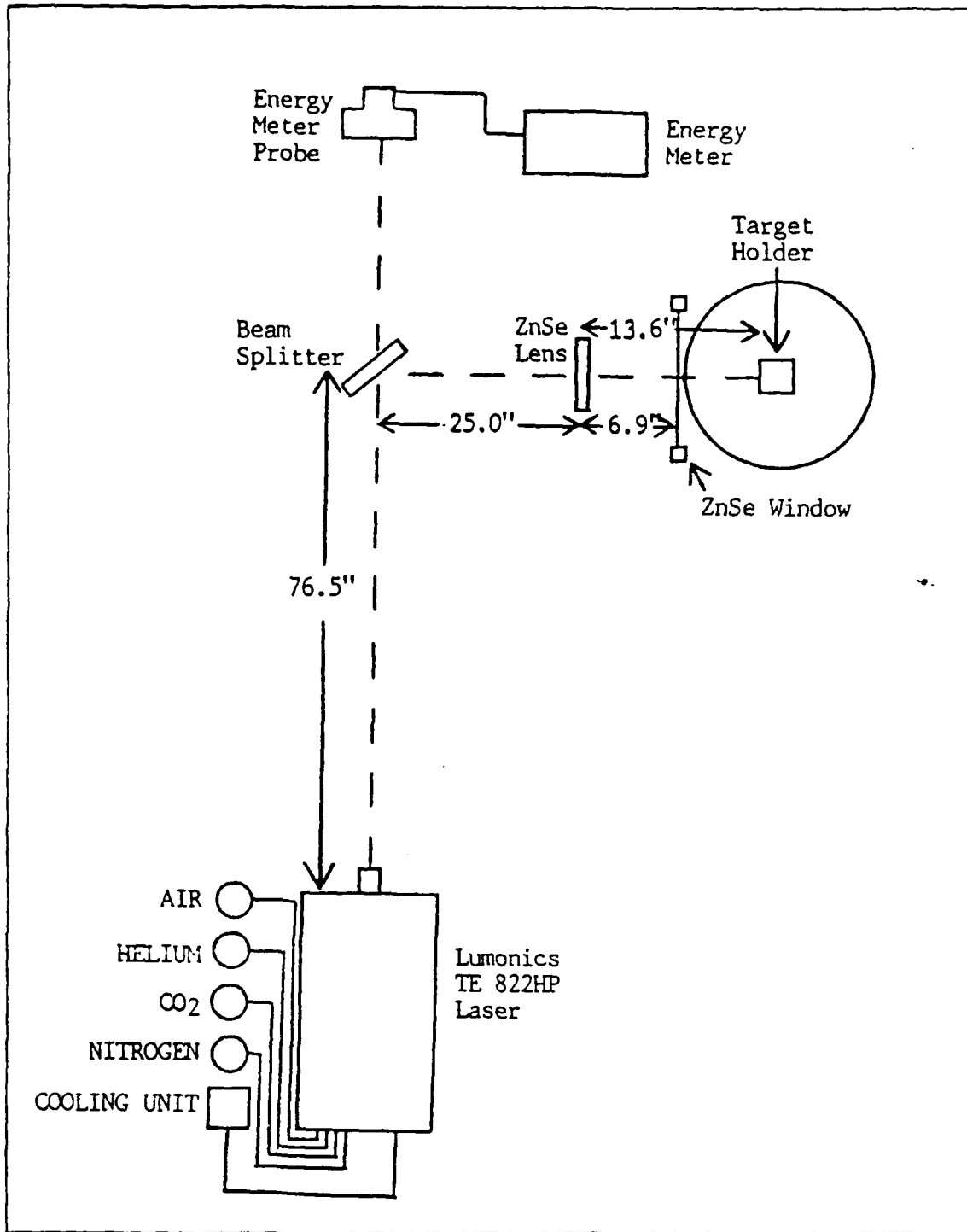


Figure 8. Experimental Arrangement

mounting it to a non-conducting phenolic holder. The copper lead was subsequently connected to the oscilloscope via a 100 to one voltage divider. Ground was established as shown in Figure 9.

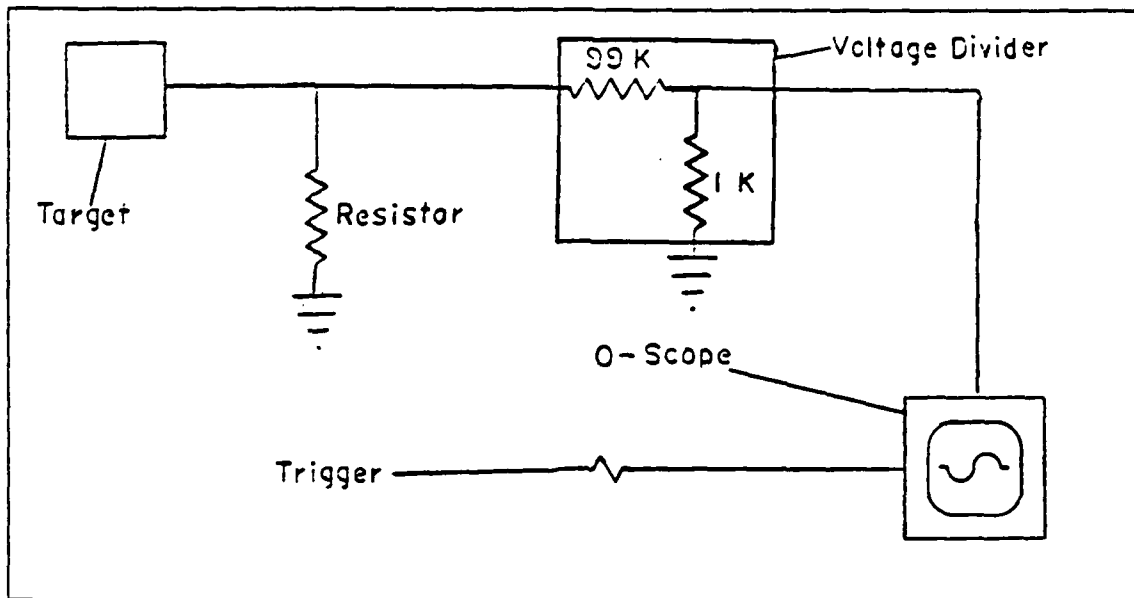


Figure 9. Circuit Diagram for Voltage Measurement

The oscilloscope was triggered via the sync-out terminal on the Lumonics Laser. This was done because the sync-out pulse was a function of the main discharge current and it was felt it provided for a sufficient triggering window for target voltage measurement.

3. Voltage, Pulse, Flash Correlation

Time correlation of the TVR, laser pulse, and flash proved to be a much more difficult and exciting endeavor. Ideally, a dual beam oscilloscope would have greatly simplified the process allowing for one beam to trace the TVR while the other traced the laser pulse or the flash and vice versa. However, the time intervals involved precluded the use of the only one available. Resorting to the single beam scope, correlation was accomplished by chopping two signals or by double and triple exposing single events.⁷ Care was taken to ensure that the leads from the laser pulse detector, flash photo-diode and target were all the same length in order to preclude introduction of systematic errors into observations with respect to timing of the events. See Figure 10 on page 20.

⁷ See results section for more information.

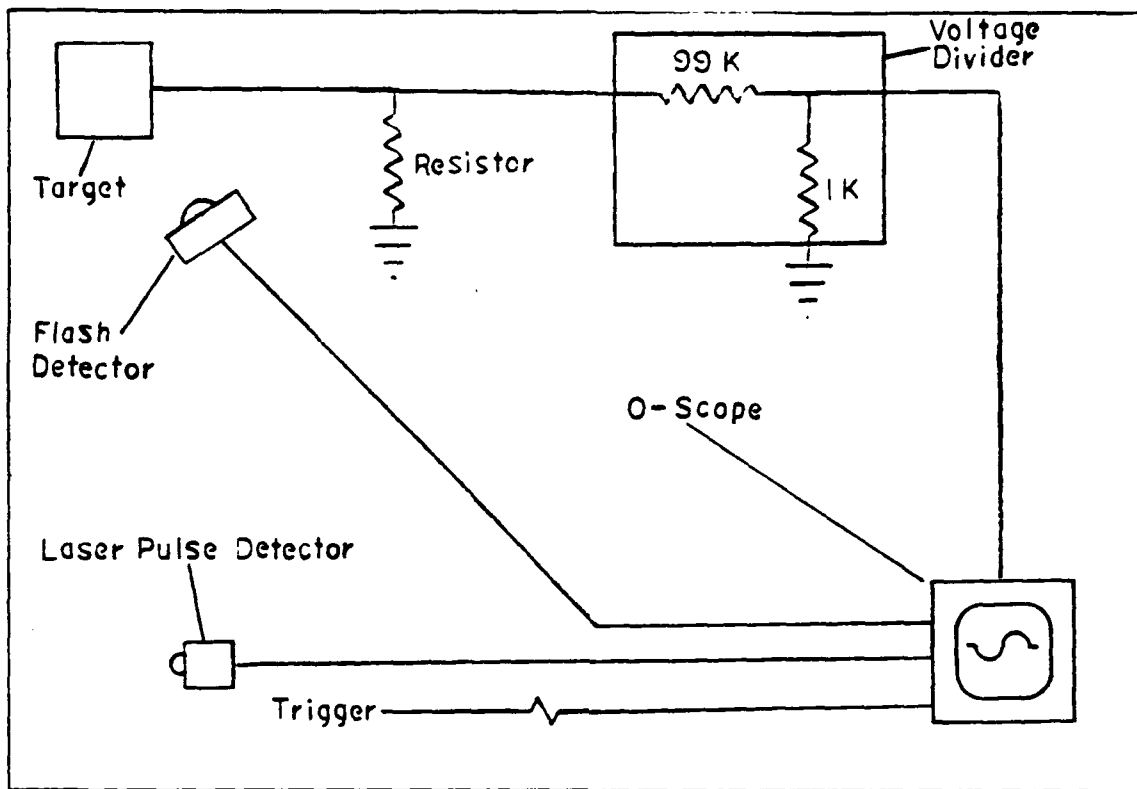


Figure 10. Circuit Diagram for Time Correlation

4. Voltage VS Pressure Comparison

To establish any pressure dependence of the voltage response, the experimental apparatus was set up in accordance with Figure 8 on page 18 and Figure 9 on page 19. Oscilloscope settings are tabulated in APPENDIX C. Pressure was measured via a Granville-Phillips vacuum gage, series 275, connected to the vacuum chamber. Units of measurement were milli-torr.

5. Current Calculations

Currents were deduced from the observed voltages and the fixed resistances to ground which varied from two mega-ohms to 0.1 ohms. Resistance to ground was reduced to less than ohm in order to encourage current flow in the case that electrons were being emitted from the target surface. See Figure 9 on page 19. Raw data for these observations can be found in APPENDIX A.

6. Energy per Pulse

The energy per pulse of the CO_2 laser was a function of the gas flow and charging current. For this experiment, settings for these parameters were kept constant for each phase. These settings are tabulated and shown in **APPENDIX C**. Ideally, the energy per pulse for the given settings should have been 15 joules per pulse. However, since observed energies per pulse varied significantly from this, it was felt that measured baseline energy per pulse should be established by recording energies for 25 shots taken over five consecutive days. This value was then used in any subsequent calculations. See **APPENDIX B** for data.

IV. EXPERIMENTAL RESULTS

A. TARGET VOLTAGE RESPONSE

The data showing how the aluminum target responded to the incident laser pulse is tabulated below. Each shot is correlated to a subsequent figure showing what was observed on the oscilloscope at the time of the event.⁸ Refer to Figure 8 on page 18 and Figure 9 on page 19 for equipment configuration. The resistance column indicates what resistance was used with respect to ground. Pulse width and voltages were taken directly from the figures presented. The voltage shown in the table is the actual voltage. That is, the 100 to one voltage divider has been taken into account. Unfortunately, the grid pattern for the scale does not appear clearly for all data presented. This was due to the short pulse duration of the TVR and the required film speed to show the sweep properly. On one hand, too much grid illumination tended to wash out the sweep. On the other hand, too little illumination showed the sweep properly, but the grid appeared weak. Occasionally, as luck would have it, a nice compromise was reached. In any case, for those figures where the grid does not show properly refer to the table for appropriate pulse width and height values.

⁸ Validation of the TVR was accomplished by shielding the target from the laser pulse during a shot and observing that the target voltage response did not occur. When the shield was removed a TVR was observed. Therefore, spurious oscilloscope pick-up was ruled out.

Table 1. TARGET VOLTAGE RESPONSE DATA

Shot	Pressure (torr)	Resistance (ohms)	Energy (J)
1	20×10^{-3}	1×10^3	14.33 ± 0.05
2	50×10^{-3}	1×10^3	13.89
3	380×10^{-3}	1×10^3	12.04
4	600×10^{-3}	1×10^3	12.51
5	5×10^{-3}	1×10^3	12.34
6	1×10^{-4}	1×10^3	14.56
7	1×10^{-4}	2×10^3	14.72
Shot	Pulse Width (ns)	Voltage (v)	Figure
1	35 ± 2	58 ± 5	10
2	24	36	11
3	18	22	12
4	20	22	13
5	40	86	14
6	41	115	15
7	30	110	16

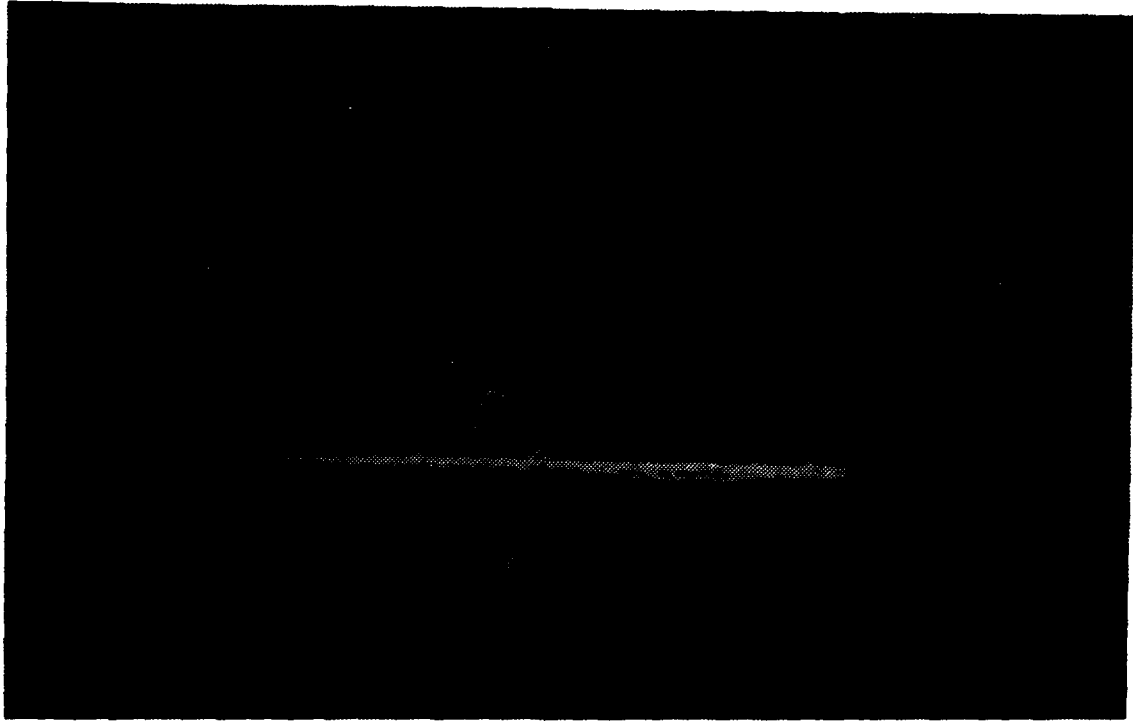


Figure 11. Voltage Response, Shot 1

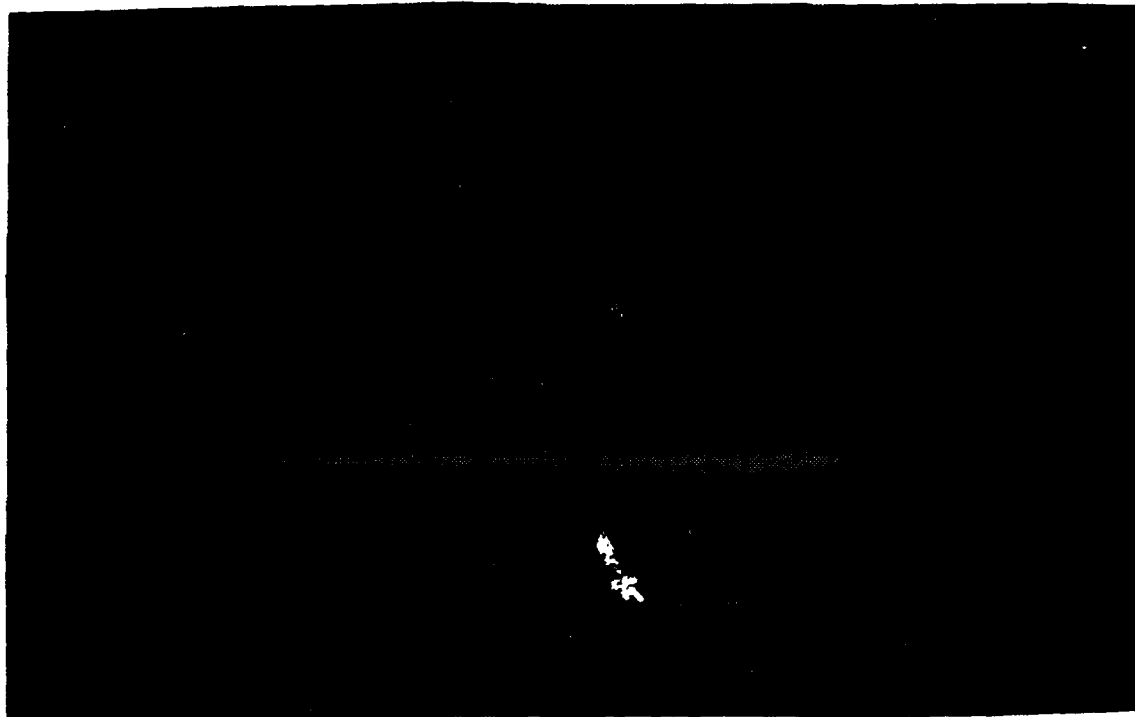


Figure 12. Voltage Response, Shot 2



Figure 13. Voltage Response, Shot 3

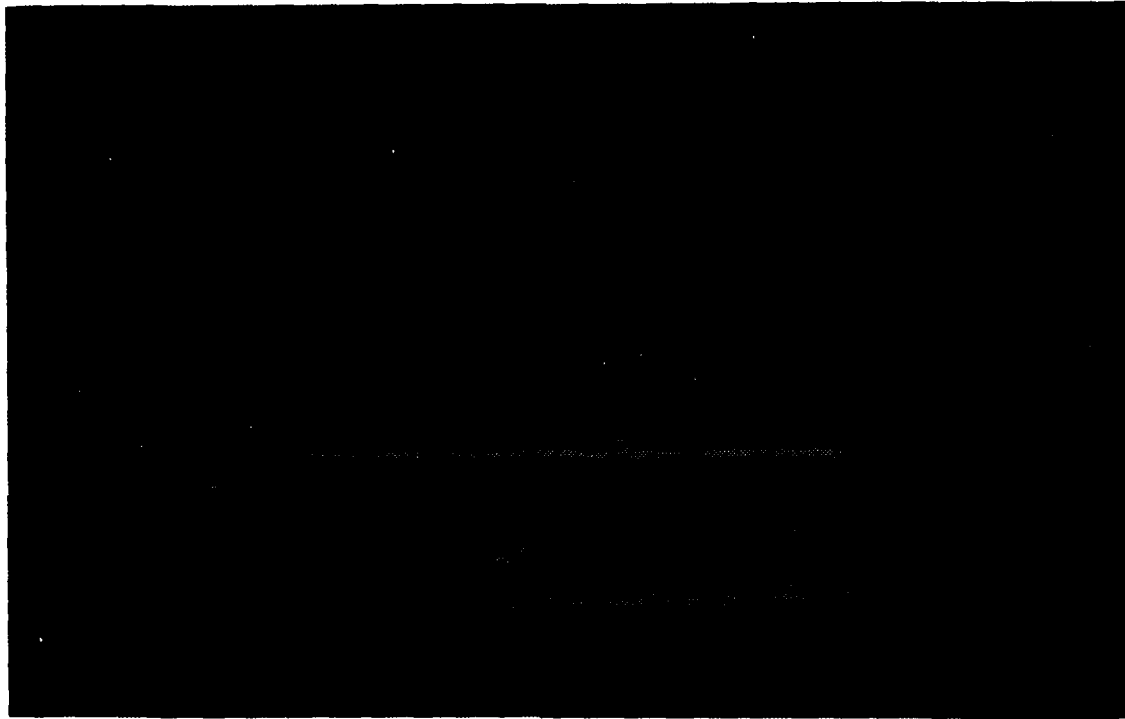


Figure 14. Voltage Response, Shot 4

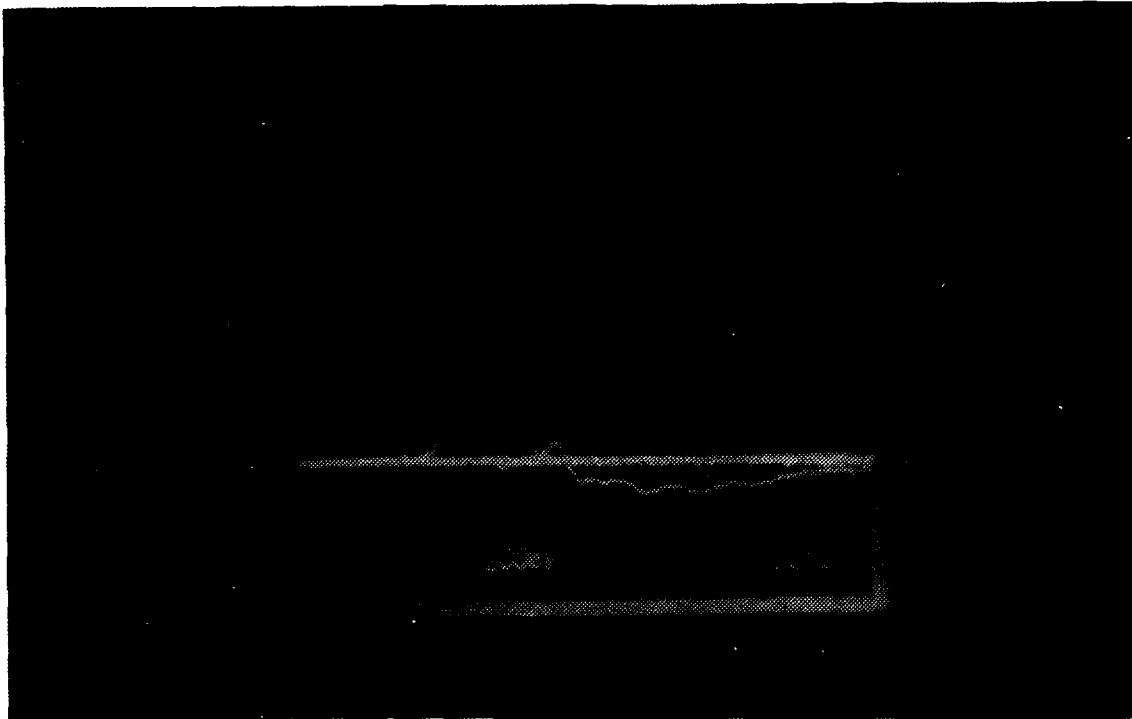


Figure 15. Voltage Response, Shot 5

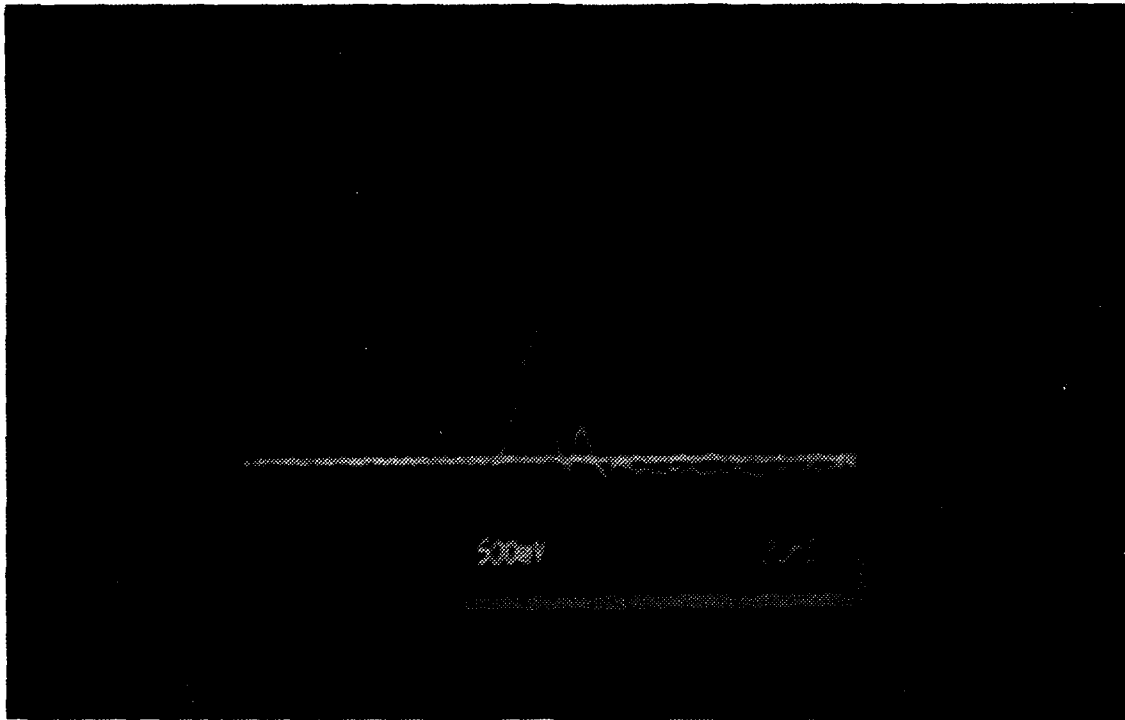


Figure 16. Voltage Response, Shot 6

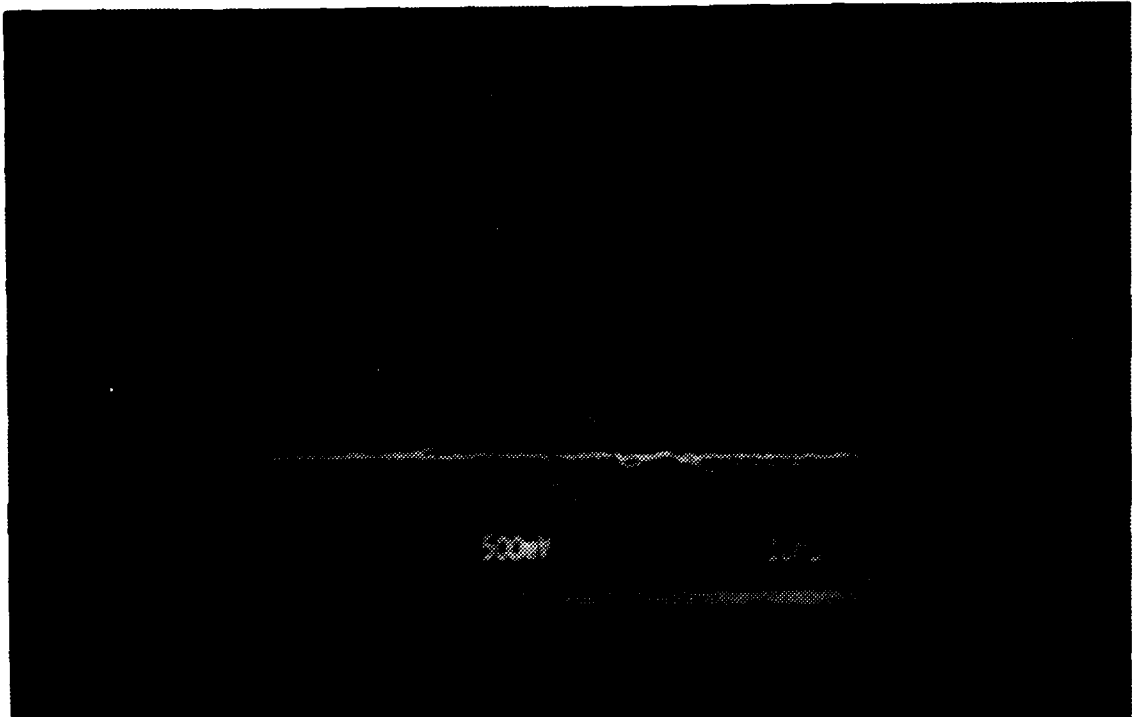


Figure 17. Voltage Response, Shot 7

B. TVR, PULSE, AND FLASH CORRELATION

Since the TVR observed and shown in part A, showed a pulse width on the order of 30 nano-seconds, it was not obvious that the time correlation of this event with the others would be possible. In other words, it was surmised that the TVR *might not show* on the time scale of the laser pulse or of the light flash. However, with much work and some luck, these correlations were accomplished with the oscilloscope in the chop mode and later via multiple exposures. For this phase of the experiment the pressure was held at 1×10^{-4} torr.

1. Chop Mode

The data for the correlation of the target voltage response with respect to the laser pulse and flash associated with target surface breakdown are presented as a sequence of figures. For this data, the oscilloscope was used in the chop mode with inputs to the scope in accordance with Figure 10 on page 20 and APPENDIX C. Table 2 presents time and voltage scales for each shot. These scales are also indicated on each figure. Vertical mode equates to voltage per division and the horizontal mode equates to time per division. Shots one through five indicate correlation of the TVR to the laser pulse. The sharp spike occurring very early, in fact immediately, in the sweep, was the TVR. The wider pulse was a representation of the laser pulse. Each subsequent shot, through five, was taken for better time resolution of the events. Hence as the time per division scale narrowed the TVR widened while the majority of the laser pulse was lost in the presentation, as would be expected. Similarly, shot 6 correlated the target surface breakdown flash with the laser pulse and, finally, shot 7 showed the TVR against the flash. LP indicated in the figures stands for laser pulse.

Table 2. VERTICAL AND HORIZONTAL MODE SETTINGS

Shot	Vertical Mode			Horizontal Mode		
	Target	Pulse	Flash	Target	Pulse	Flash
1	500 mv	500 mv		1 μs	2 μs	
2	100 mv	500 mv		1 μs	1 μs	
3	500 mv	500 mv		500 μs	500 μs	
4	500 mv	500 mv		100 μs	100 μs	
5	500 mv	500 mv		50 ns	50 ns	
6		500 mv	100 mv	1 μs		1 μs
7	200 mv		200 mv	2 μs		2 μs

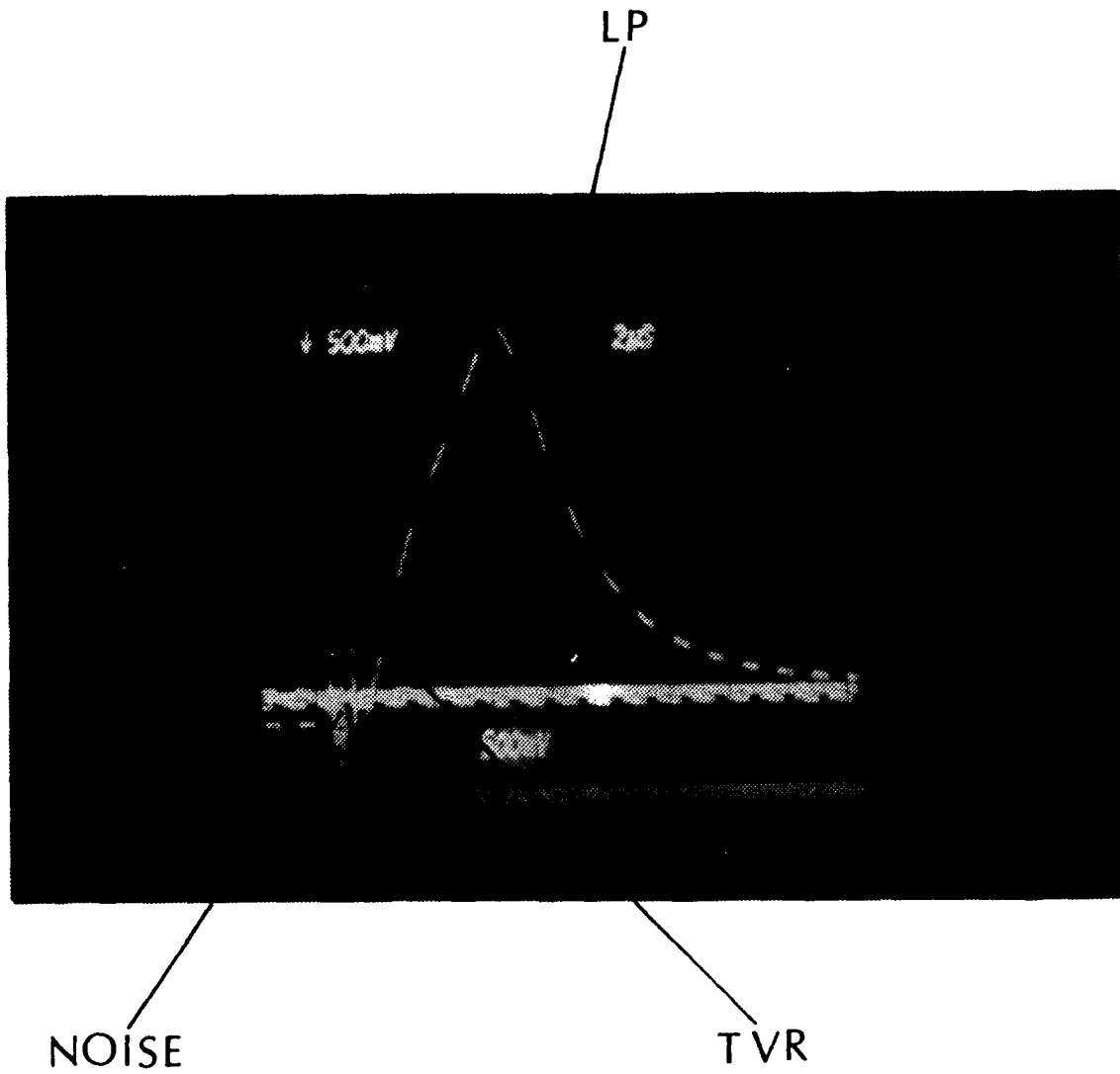


Figure 18. TVR and Laser Pulse, Shot 1

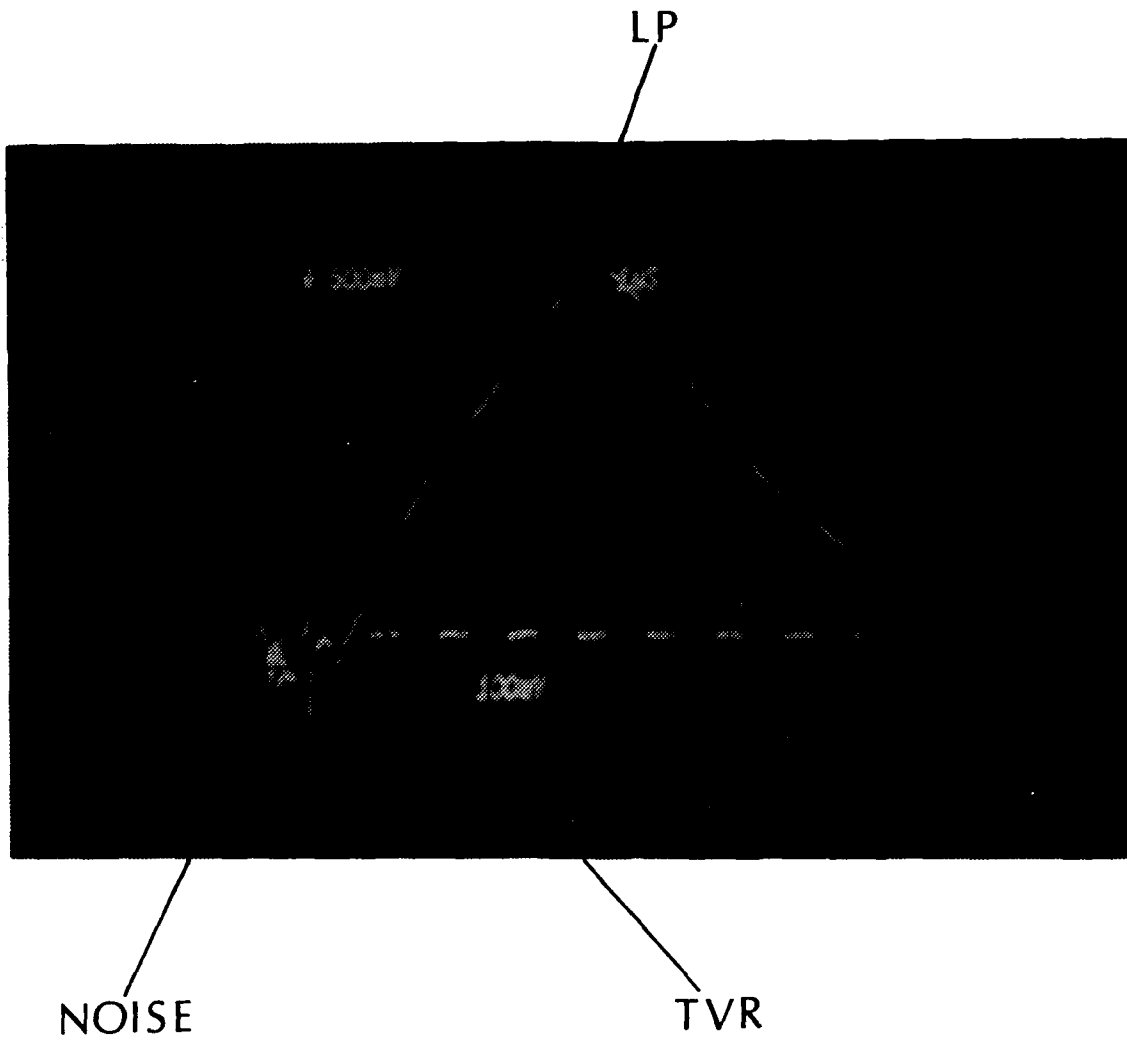


Figure 19. TVR and Laser Pulse, Shot 2

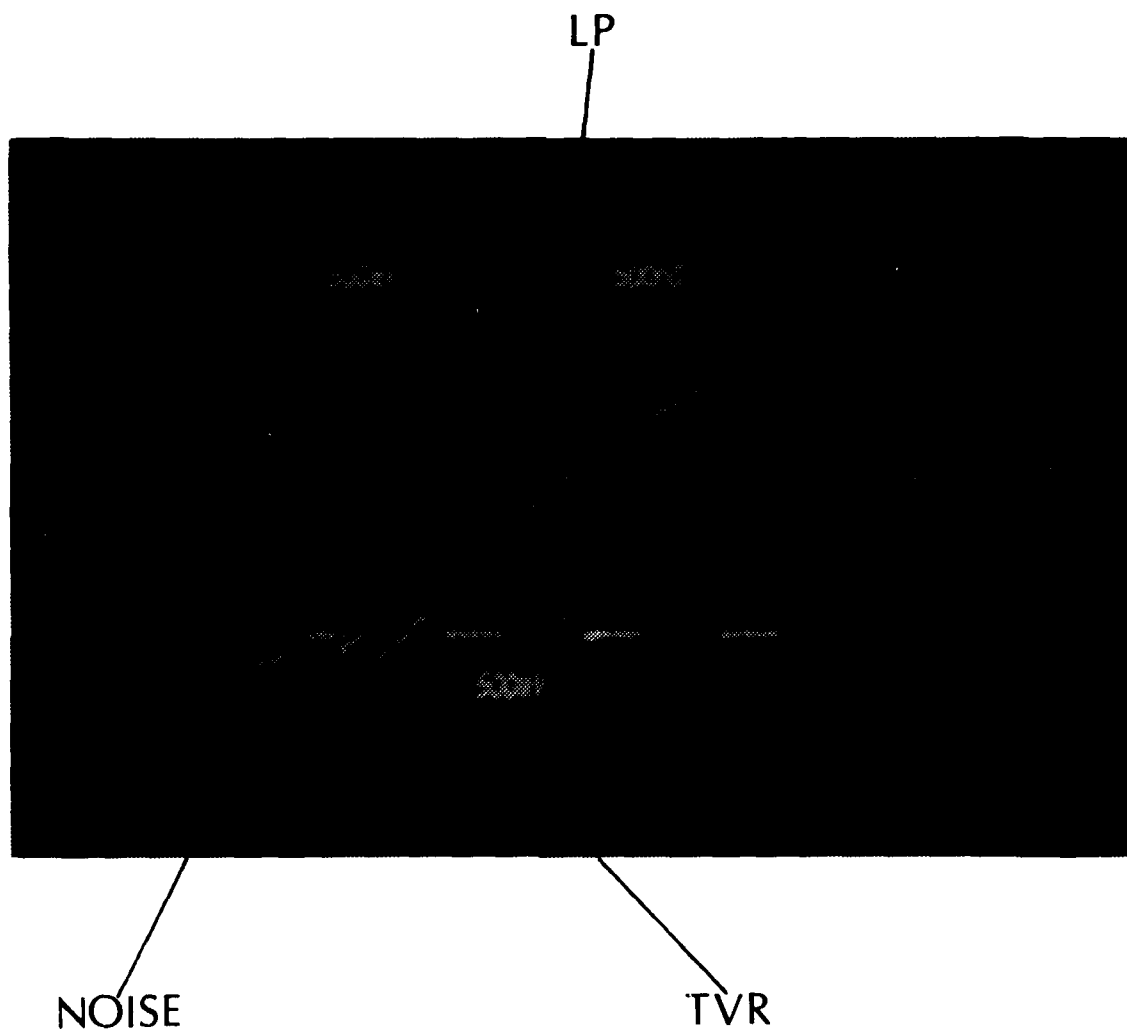


Figure 20. TVR and Laser Pulse, Shot 3

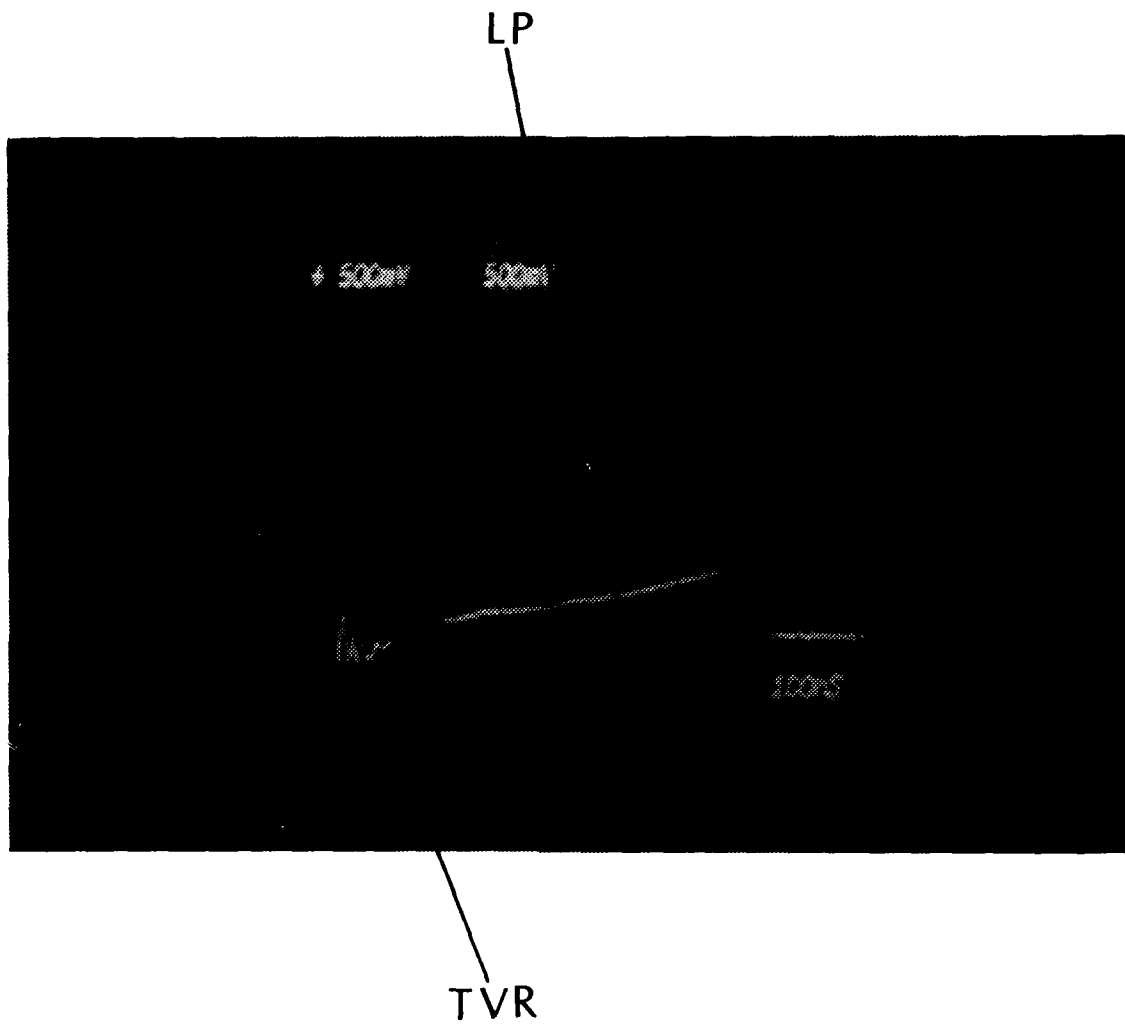


Figure 21. TVR and Laser Pulse, Shot 4

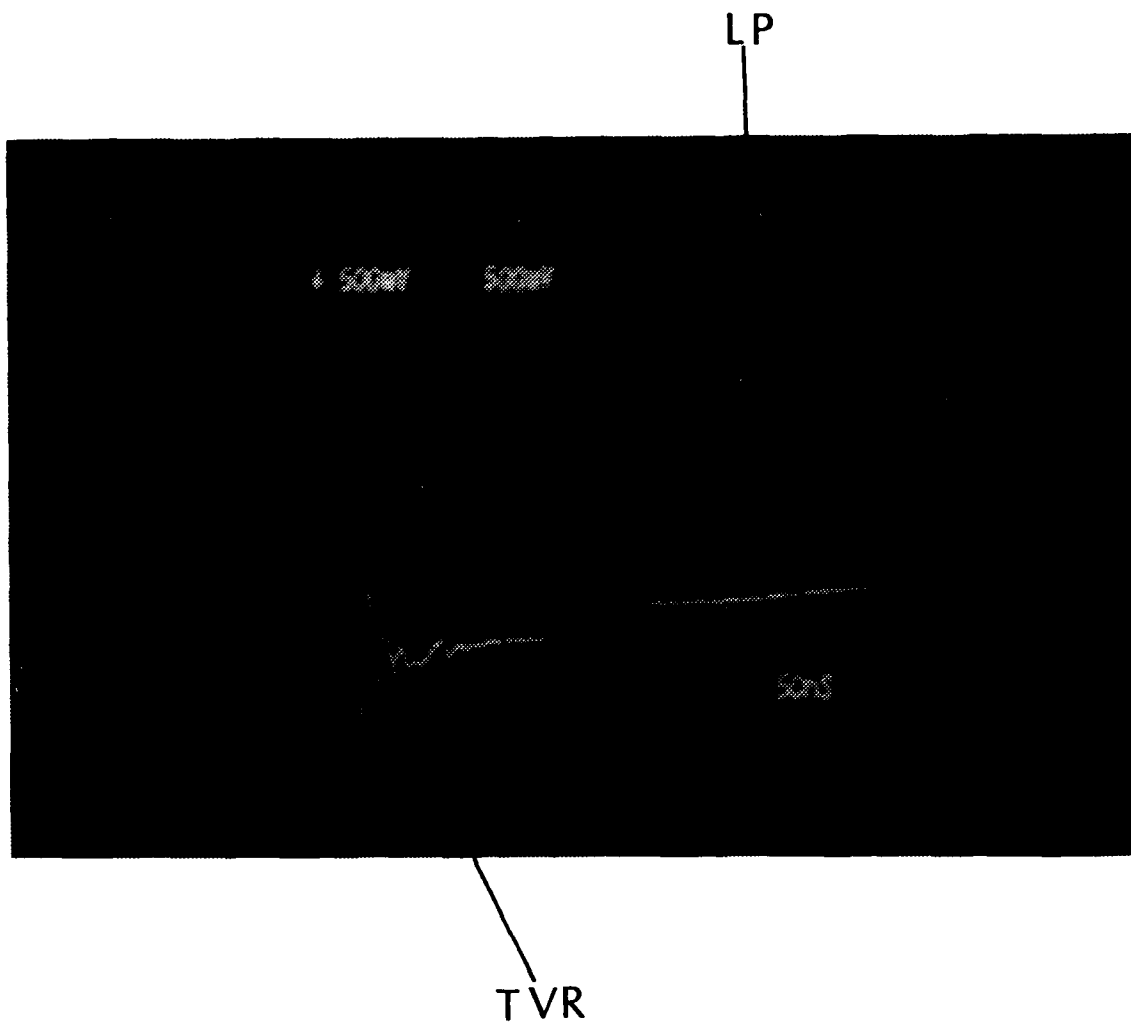


Figure 22. TVR and Laser Pulse, Shot 5

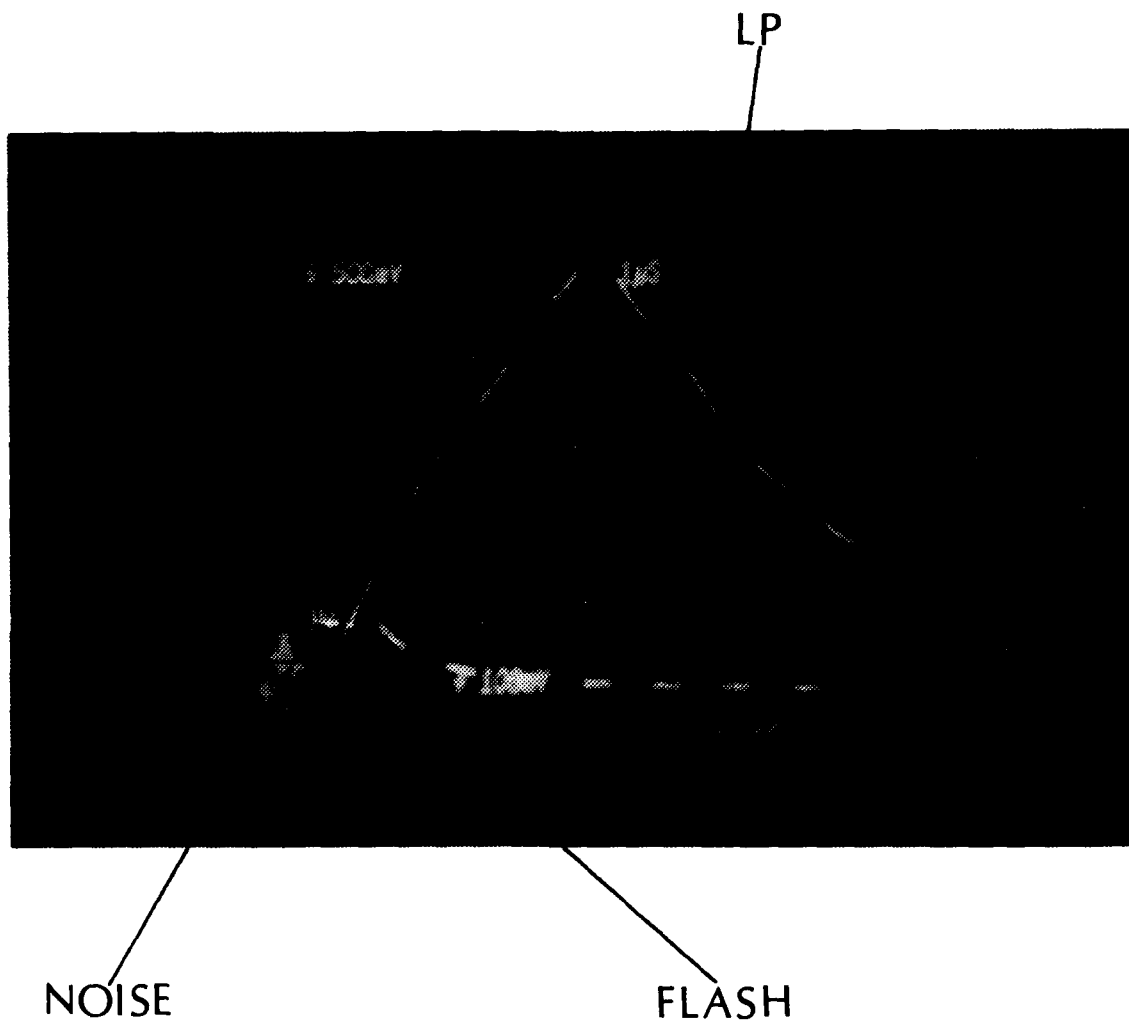


Figure 23. Flash and Laser Pulse, Shot 6

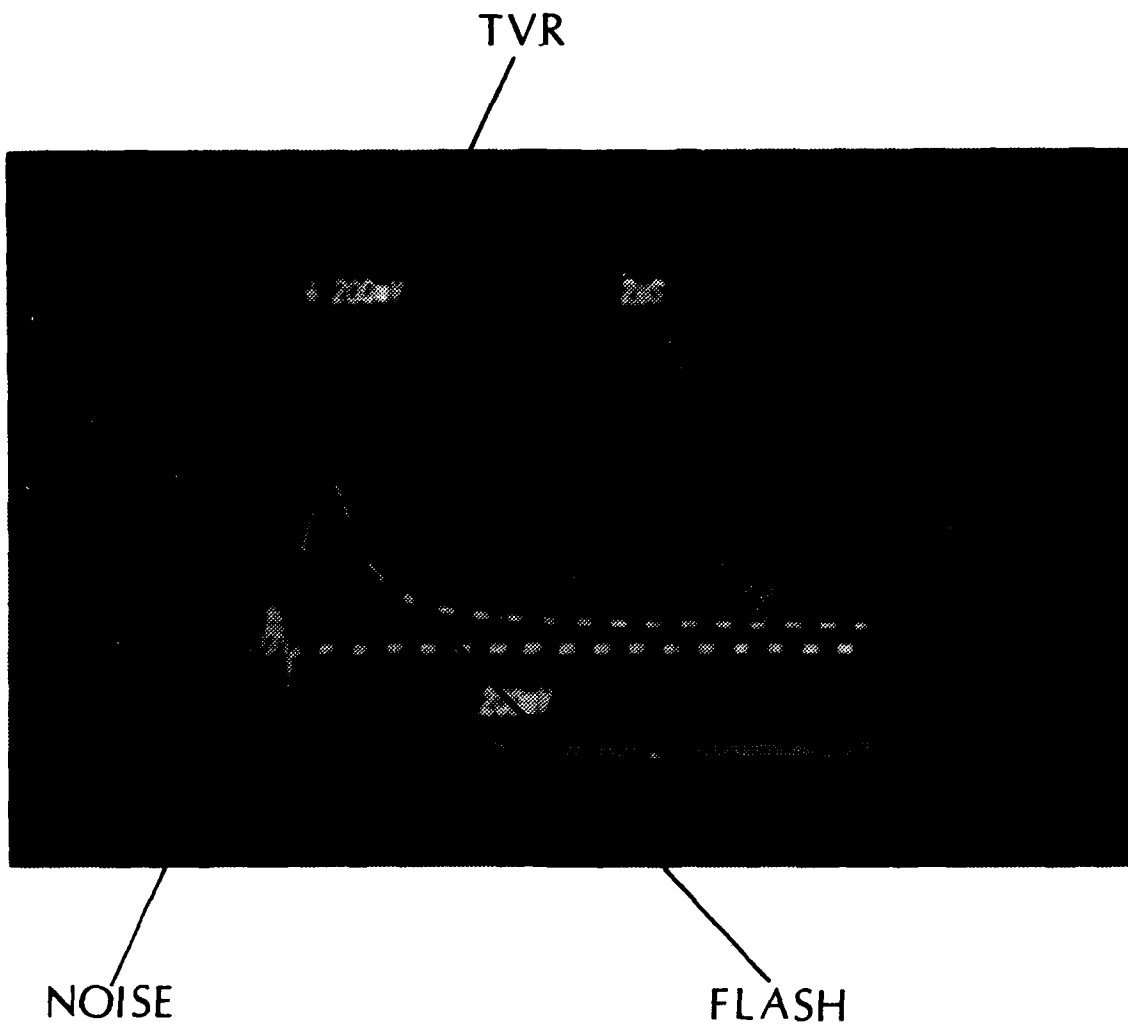


Figure 24. Flash and TVR, Shot 7

2. Multiple Exposures

Since the chop mode gave a respectable, albeit qualitative, showing of the time relationship between these three events, it was felt that information was being lost in the gaps of the chop. In fact, it appeared, unbelievably, that the TVR occurred prior to the arrival of the incident laser pulse, see Figure 21 on page 35 and Figure 22 on page 36. It was decided that a multiple exposure of these single events would give insight into what was being observed. Therefore, the next four figures show the TVR, the laser pulse, the flash, and the superposition of all, respectively. The vertical and horizontal modes for the oscilloscope were 100 milli-volts and 200 nano-seconds as is indicated on each figure. These data show a quantitative relationship between the events. The superposition of the single events indicated that the TVR and the flash associated with target surface breakdown occurred approximately 200 nano-seconds into the laser pulse. Refer to figure 28. It was noted that the first response of the laser pulse sweep was negative, see Figure 26. This was attributed to a reverse voltage bias in the amplifier of the laser pulse detector.

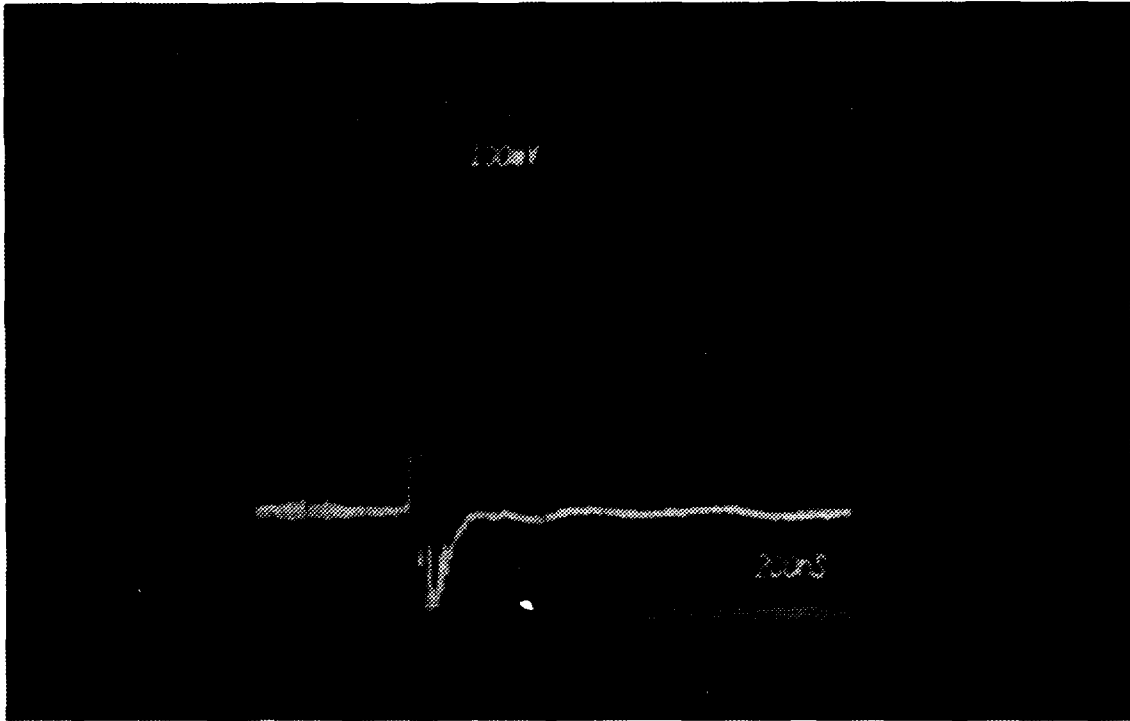


Figure 25. TVR, Shot 1

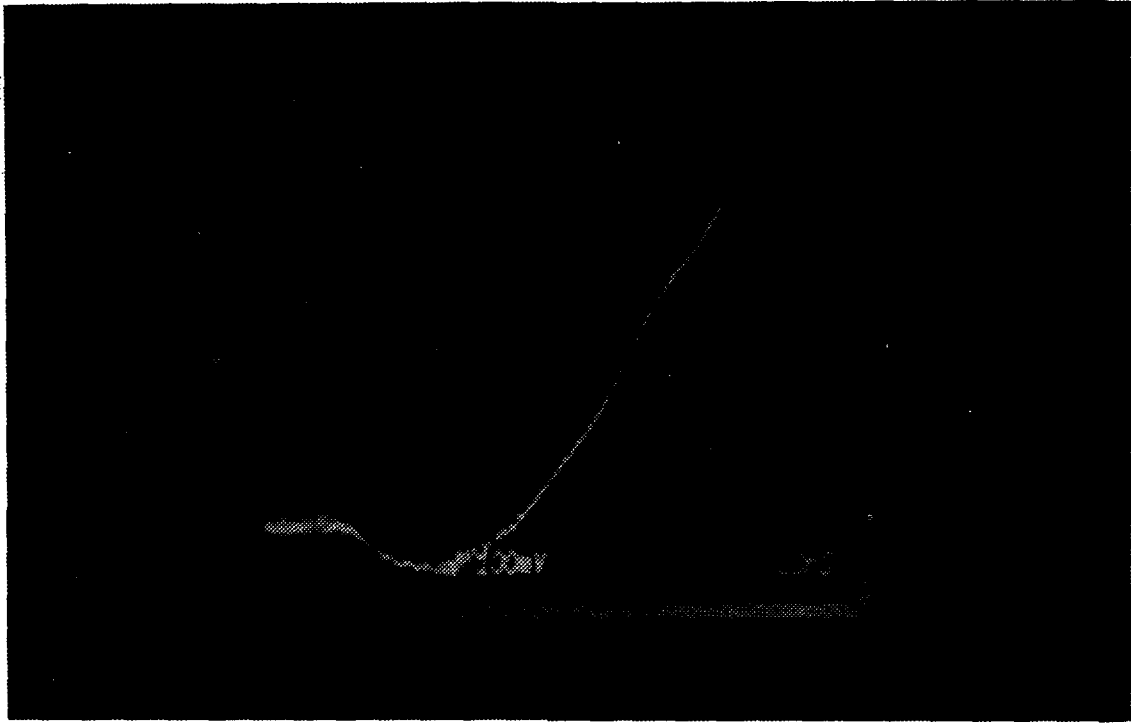


Figure 26. Laser Pulse, Shot 2

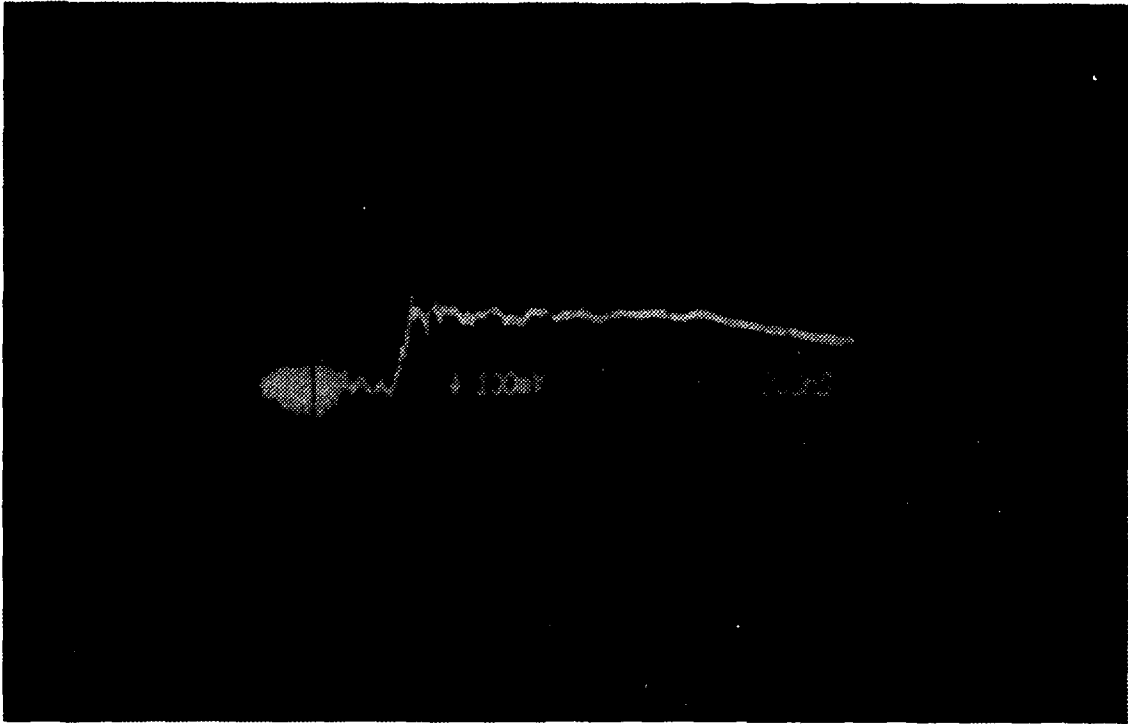


Figure 27. Flash, Shot 3

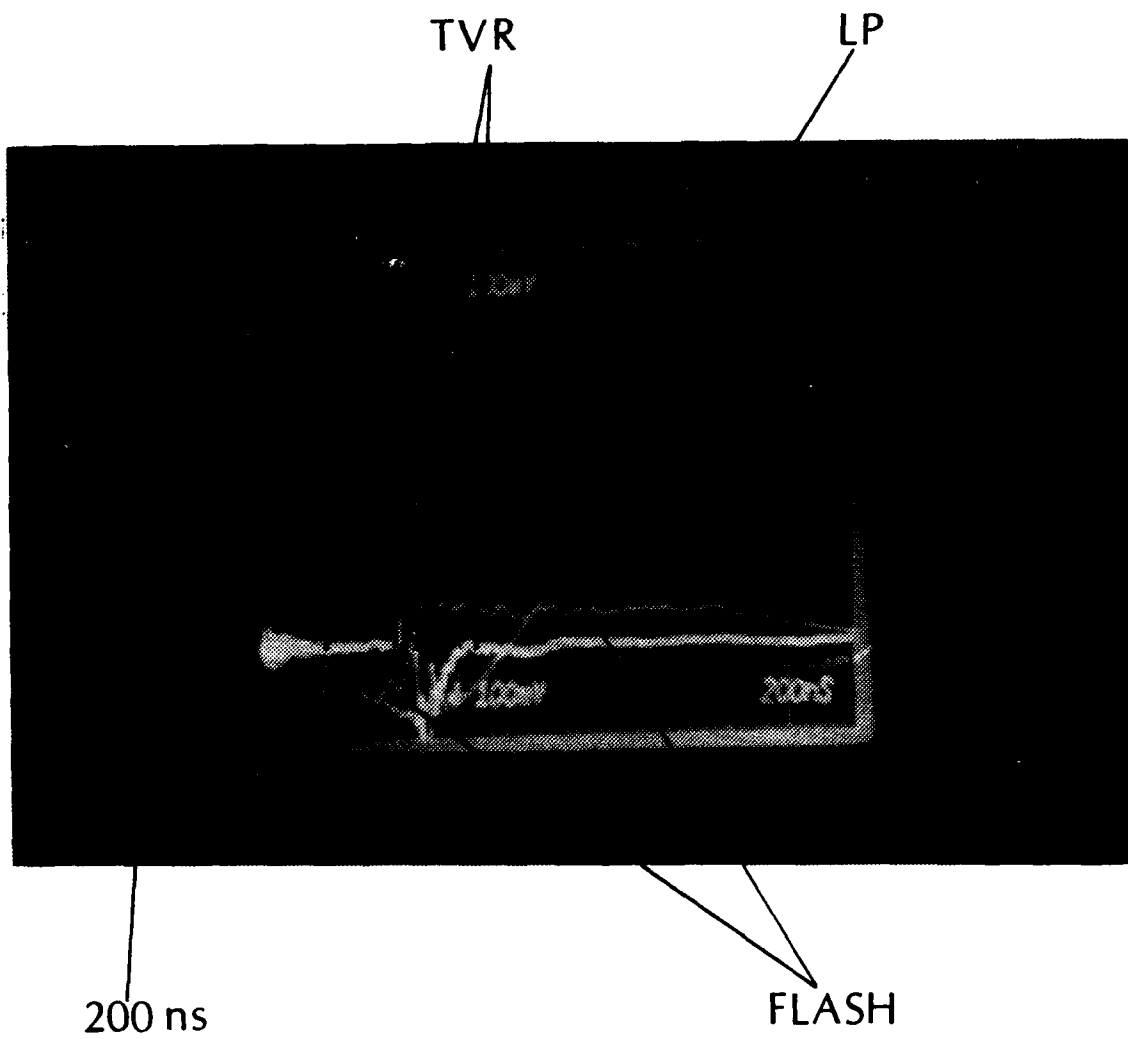


Figure 28. TVR, Laser Pulse, Flash, Shot 4

C. PRESSURE DEPENDENCE OF THE TVR

Data contained in Table 1 on page 20 in association with Figures 10-16 on pages 21-22, indicated that the magnitude of the voltage response was indeed a function of, or dependent upon the background gas pressure. In order to see this relationship more clearly, a voltage vs pressure graph is presented in Figure 29. Notice that the data point from shot 7 is not used since the resistance to ground was not consistent with the others.

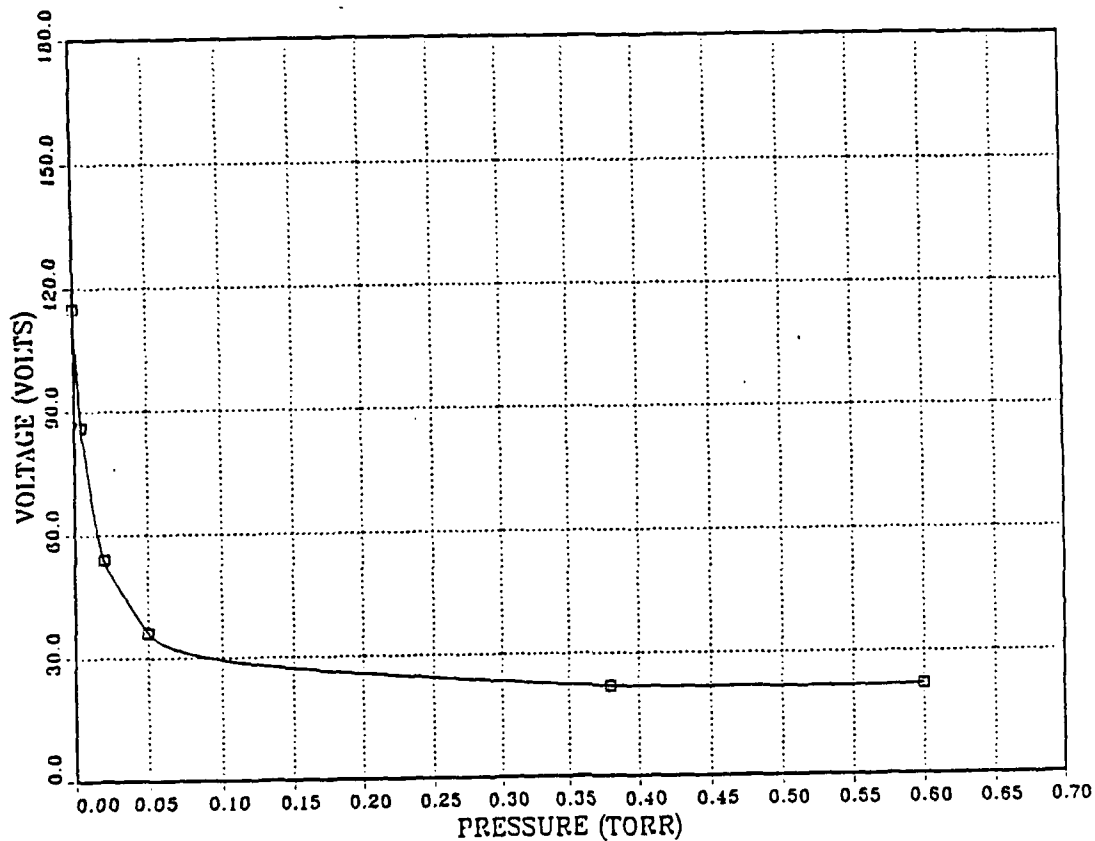


Figure 29. Voltage vs Pressure Relationship

D. CURRENT DEDUCTIONS

Deduction of the currents associated with a given voltage pulse were obtained from *Ohm's Law*,

$$I = \frac{V}{R}. \quad (19)$$

The data for this phase of the experiment is contained in **APPENDIX A** . Voltages were observed as indicated on the oscilloscope. The controlled parameter was the resistance to ground and was varied from two mega ohms to 0.1 ohms. Figure 9 on page 19 shows how and where, in the circuit, ground was established. Figure 30 shows the entire spectrum of data with resistance plotted, on a log scale, against the current. Subsequent figures expand these data for a closer view. Figure 31 presents the data from resistances of two mega ohms to 110 ohms. Figure 32 shows the relationship from 36 to 15 ohms. Figure 33 consists of data from one to 0.1 ohms.

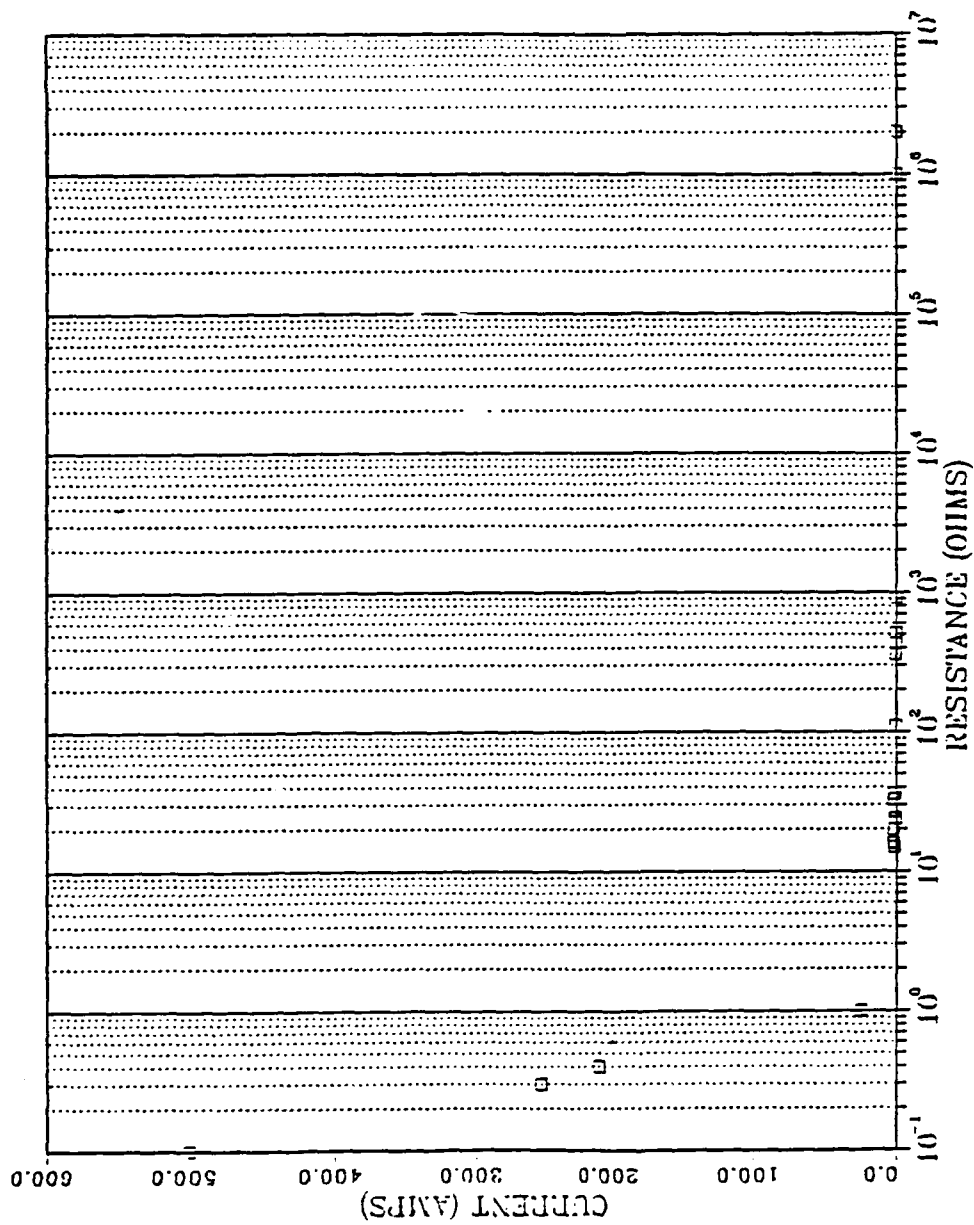


Figure 30. Current vs Resistance, Log Scale

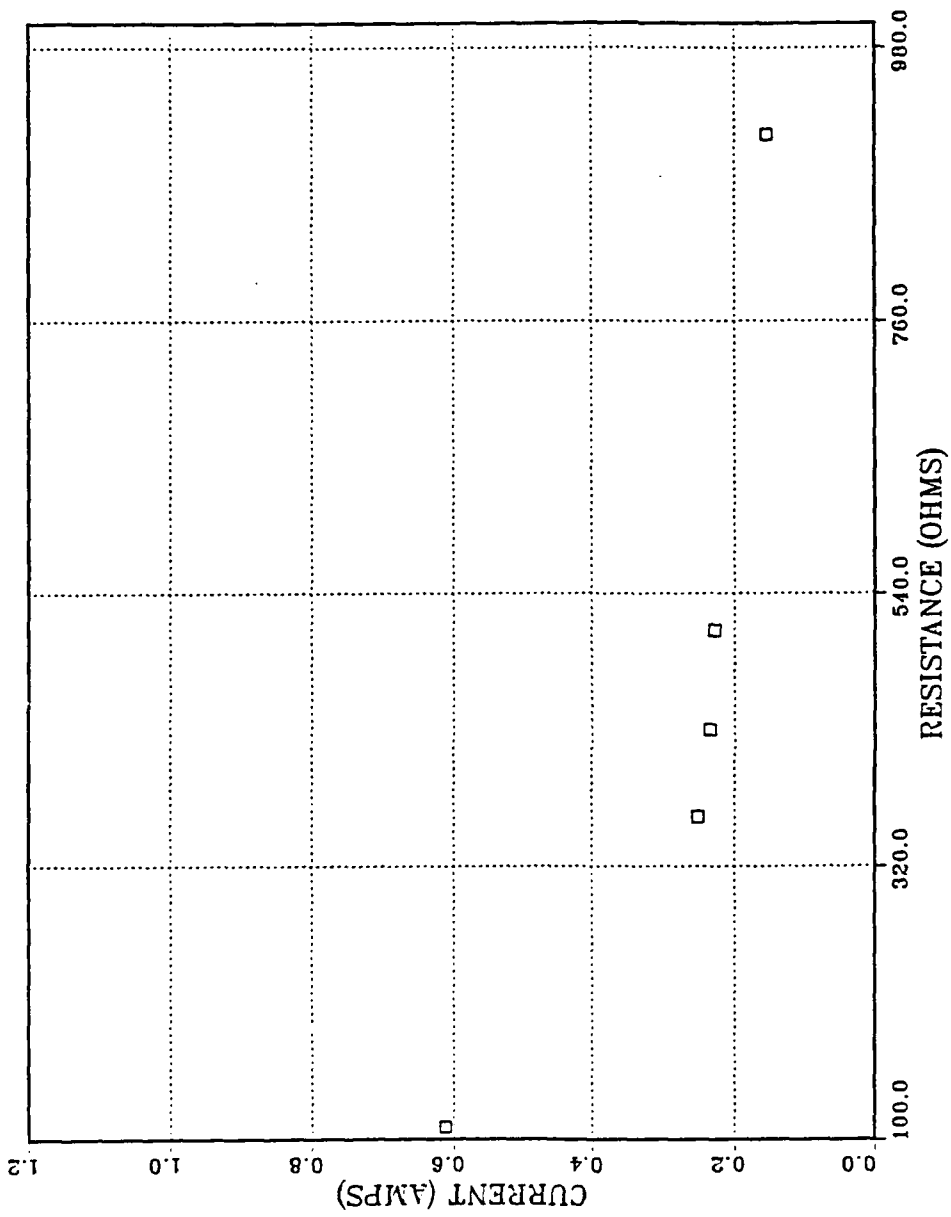


Figure 31. Current vs Resistance, Two Mega-Ohms to 110 Ohms

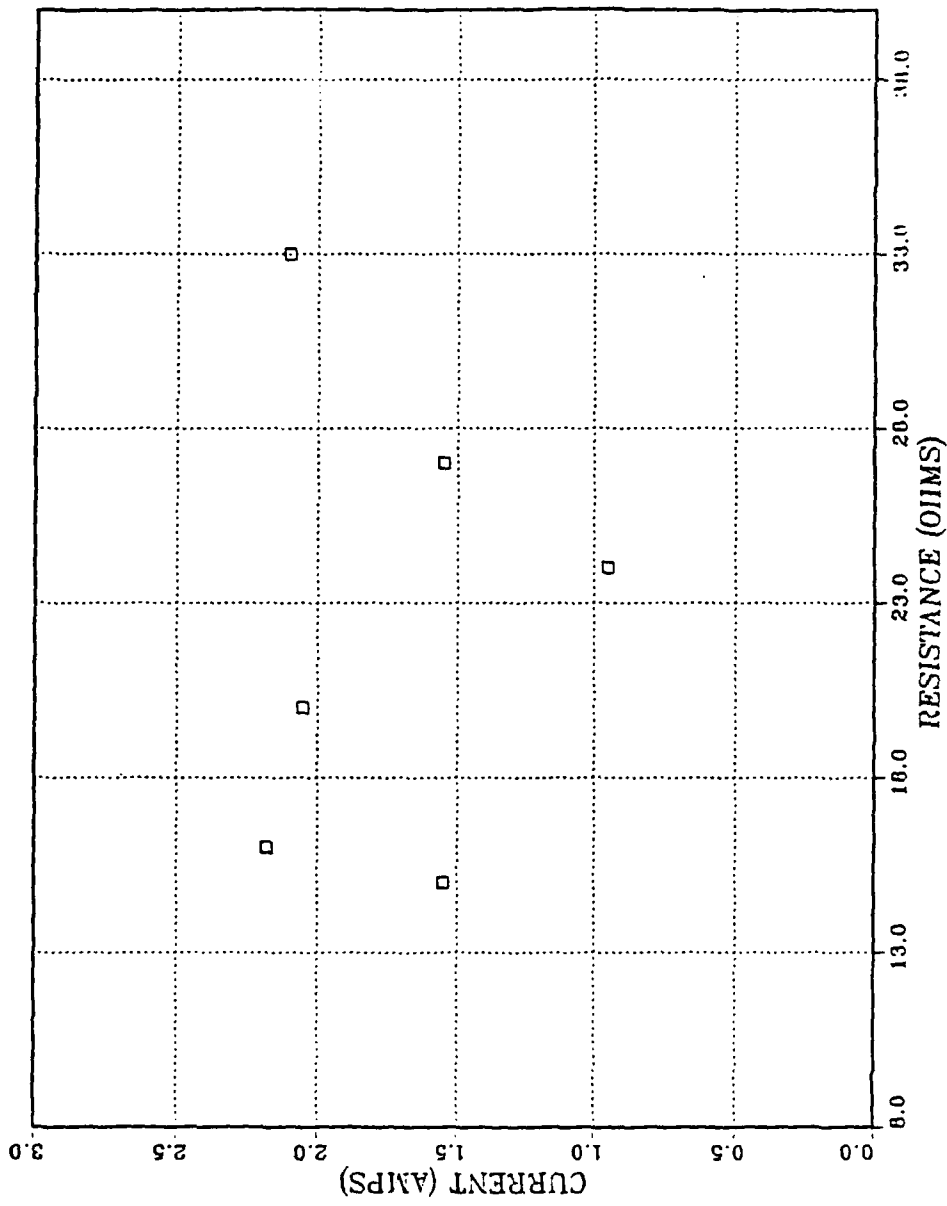


Figure 32. Current vs Resistance, 36 to 15 Ohms

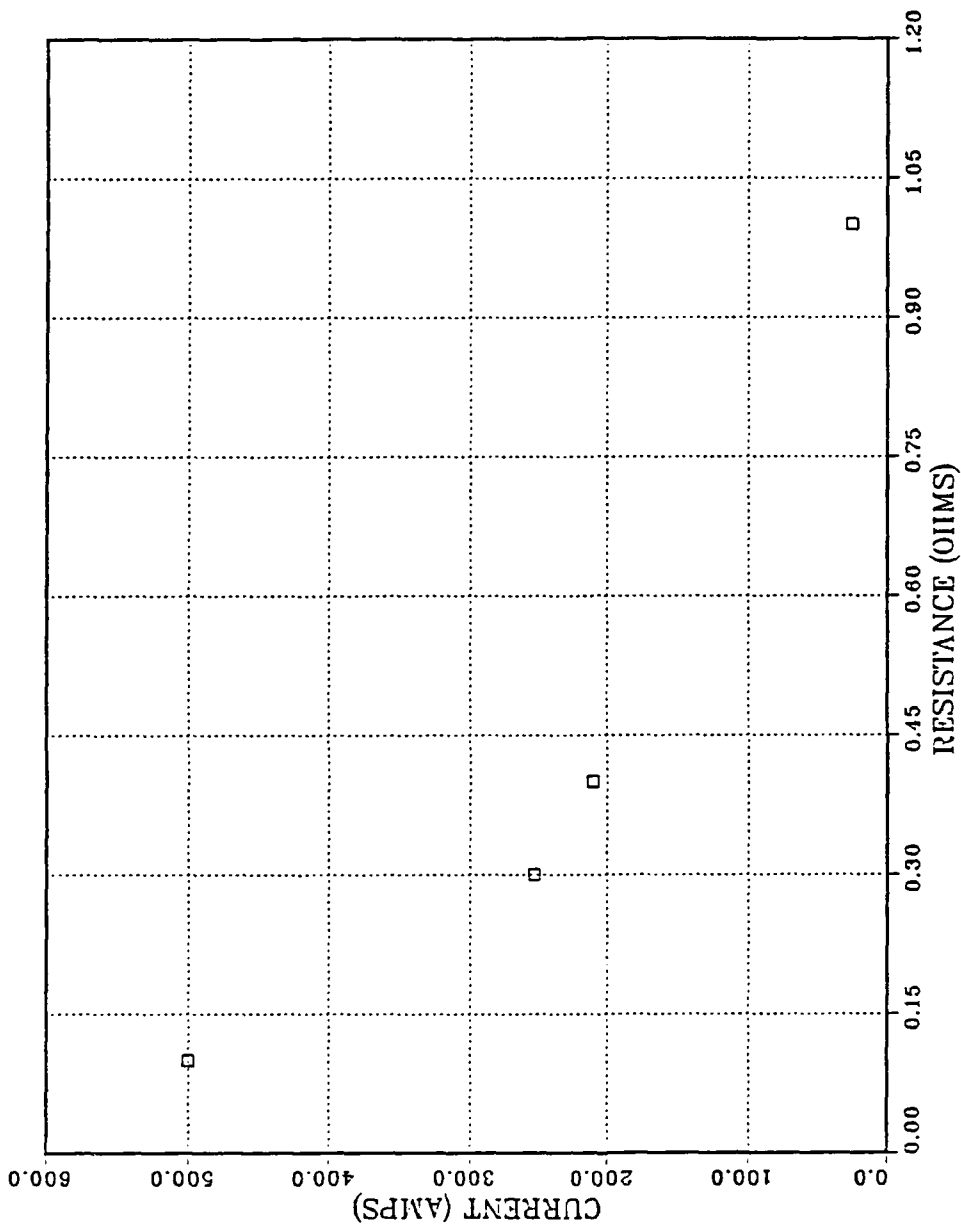


Figure 33. Current vs Resistance, 1 to 0.1 Ohms

V. ANALYSIS OF DATA

A. DATA CHARACTERISTICS

The following characteristics of the TVR and associated events were noted.

- In all cases, the voltage response was initially positive (Figures 11-17).
- At lower pressures less than 50 torr, the TVR showed a unique double spike phenomenon (Figures 11,15,16 and 17).
- The magnitude of the TVR was inversely proportional to the background gas pressure (Figure 29).
- In all cases, the initial positive spike was followed by a *residual* negative potential (Figures 11-17).
- The TVR occurred 170 nano-seconds into the laser pulse (Figure 28). See **Appendix D** for calculation.
- The TVR and the flash associated with surface breakdown occurred at the same time (Figures 24 and 28).
- The maximum target current induced was 500 amps (Figures 30-33).
- The mean pulse width of the TVR was calculated to be ≈ 30 nanoseconds.

B. DISCUSSION

1. TVR Measurement, Electron Emission

Interpretation of the TVR proved difficult. The positive nature of the initial voltage spike, certainly implied that the target had emitted electrons from the surface. However, the explanation of how this occurred was not easy. Photo-emission was immediately ruled out due to the low photon energy of the CO_2 laser. Initially, it was felt that thermionic electron emission was possible due to the fact that nine electron volts per atom of laser energy could be deposited to the first layer of atoms in the focal spot area on the target. This would occur in the 170 nano-seconds prior to the TVR and subsequent electron emission. See **Appendix D** for details. However, this argument failed when reflectivity, heat conduction, and skin depth were accounted for. For example, Schriempf [ref. 10] showed that the absorptivity of 2024 aluminum at room temperature was only 0.03 at $10.6 \mu m$. Taking this into account, the energy per atom rapidly fell below 1 electron volt,⁹ ruling out the possibility of thermionic emission. This also

⁹ The work function for aluminum is 4 electron volts.

ruled out Schottky emission since this mechanism is mainly thermionic, enhanced by an external electric field.

In order for field enhanced emission to work, electric fields on the order of $\sim 10^6$ volts per centimeter must be established [ref. 4]. Integration of the laser pulse from initiation to 170 nano-seconds, gave an energy value of 1×10^{-4} joules, and an irradiance of 666.6 watts per square centimeter, which would correspond to a wave electric field of $\sim 10^3$ volts per centimeter. This value is too low. However, if surface features are taken into account, field enhanced emission could work. For example, assuming that a few electrons are already present at the distance $\frac{\lambda}{4}$, then ionization of some neutrals would occur. For convenience, these first few electrons can be defined as *anomalous free electrons*. Any plasma ions created near $\frac{\lambda}{4}$ would be subject to a pressure gradient and an associated ambipolar electric field,

$$E = - \frac{\nabla P_e}{en}.$$

This equation is derived from the fluid equation of motion [ref. 7]. The assumptions are that a first order, steady state condition exists where the magnetic field is zero. This pressure gradient would cause some ions to move toward the target surface. Due to the non-uniform nature of a surface whisker and its associated electric field, a concentration of ions would occur near it. This would, in turn, create a local increase in the sheath electric field. Since field emission increases sharply with an increase in electric field, a sharp onset of electron emission would occur. Therefore, the target would charge positive with respect to the vacuum chamber, as the TVR indicates. So, it was proposed that field enhanced emission caused the burst of electrons from the target. Of course, the assumption that a few *anomalous free electrons* were already present was necessary.

The proposed sequence of events is as follows.

- The laser pulse strikes the target causing immediate desorption of contaminants and an expanding neutral gas.
- An electromagnetic standing wave is established due to the superposition of the incident and reflected waves.
- *Anomalous free electrons* interact with the standing wave causing ionization of some of the expanding neutrals.
- Some ions move toward the target due to the electric field caused by pressure gradients normal to the surface.

- A concentration of these ions around a surface whisker, Figure 6, results in a local increase in the sheath electric field and subsequently causes field enhanced emission.
- The sudden emission of electrons from the surface produces the observed TVR. The escape of a few very fast electrons from the plasma results in both, the target and the plasma in front of the target, assuming a positive potential with respect to the surrounding vacuum chamber. It should be noted that the sheath between the plasma and the target still exists, with the plasma being more positive than the target.
- The injection of electrons into the plasma, and the intense heating of electrons in the $\frac{\lambda}{4}$ region, causes rapid plasma growth to the critical density.
- The build-up of the plasma density near the whisker, leads to further electron emission. The whisker explodes and a Unipolar-arc forms.

Since the floating potential V_f , equation (10), requires that the target be negative with respect to the plasma in contact with it, the residual negative potential of the TVR is interpreted to mean that the plasma has reached critical density and is interacting with the target surface. See Figure 34.

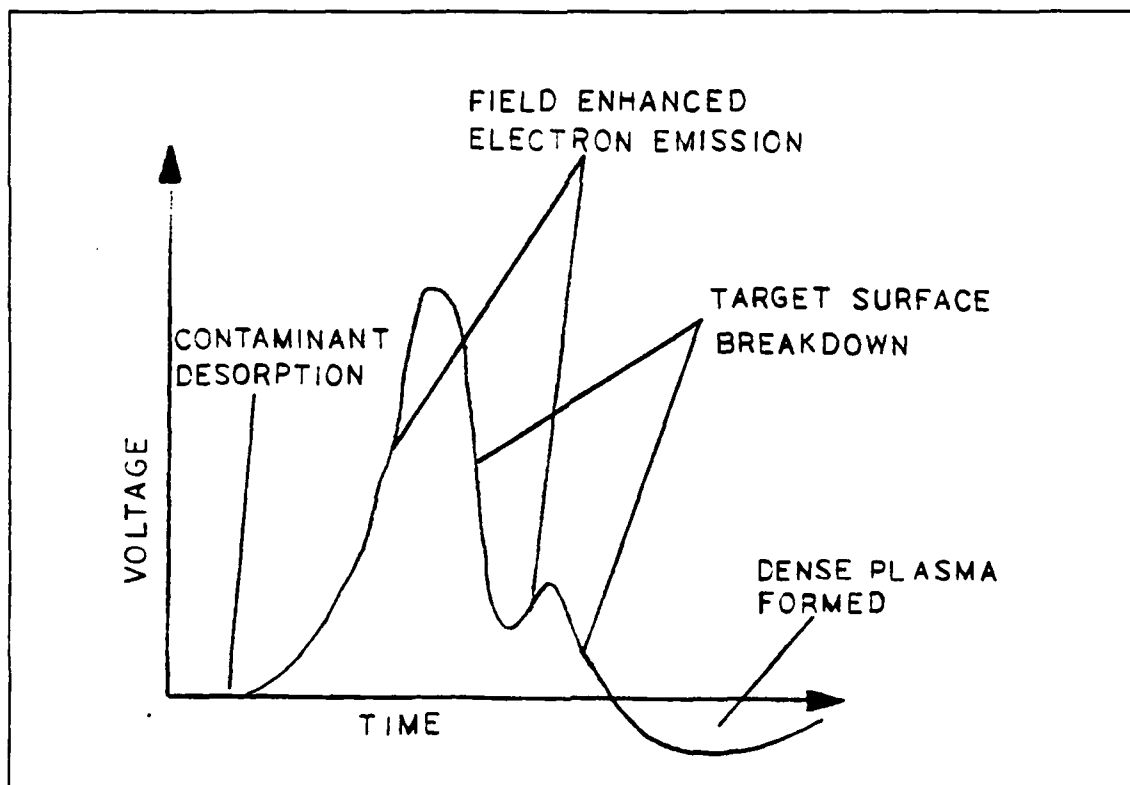


Figure 34. Characteristics of the TVR

2. TVR, Laser Pulse, Flash correlation

Correlation of the TVR with the laser pulse showed that a voltage response occurred approximately 170 nanoseconds into the laser-target interaction. Similarly, correlation of the TVR with the target surface breakdown flash showed that it was the beginning mechanism for plasma creation. These characteristics suggested an ignition and transition process for a LSD wave as defined on page eight. The TVR, electron emission from the target, would equate to the ignition mechanism, while the flash would equate to a transition mechanism. Both are consistent with reported LSD wave properties. Furthermore, data Walters gathered on LSD wave phenomena, supports this assertion. First of all, he indicated that LSD waves were ignited from " ...numerous luminosity sites... " on the target surface [ref. 5]. An initial electron burst from a target whisker could correspond to a luminosity site. Also, Walters reported that laser irradiances of $10^7 \sim 10^8$ watts per square centimeter, from a 75 joule, TEA CO_2 laser on aluminum targets, initiated LSD waves in atmospheric pressure. He further reported that LSD ignition occurred 50 nanoseconds into the laser pulse [ref. 5]. For this experiment, based on a 0.09 square centimeter focal spot area, a pulse irradiance of 2.8×10^7 watts per square centimeter was calculated. See Appendix D for details. The differences in ignition response times, 50 nanoseconds vs 170 nanoseconds, is attributed to this experiment being conducted in vacuum as opposed to atmospheric pressure. Therefore, the desorption process prior to the TVR would delay the occurrence of LSD ignition. At atmospheric pressure the neutral density, required for LSD ignition via enhanced field emission, would already exist. [ref. 5]

3. Current Deductions

The initial objective of this experiment was accomplished in that the currents induced by incident laser radiation were quantitatively established. When resistances to ground were high, the associated currents were small. On the other hand, a current of 500 amps was calculated at a resistance of 0.1 ohms. The reason for this result can be qualitatively explained as follows. When electrons are initially emitted from the target, the target surface immediately assumes a positive potential. For cases where resistance to ground is high, the magnitude of the positive potential is such that all but the most energetic electrons are drawn back to the surface and only a few escape to the vacuum chamber wall to complete the circuit. Therefore, the currents are small. On the other hand, when resistance to ground is small (less than one ohm) the magnitude of the positive potential is such that more electrons can escape to the vacuum chamber wall resulting in larger currents.

A recommendation for further research is suggested to determine if an electromagnetic pulse is the result of such a current. Certainly, a $\frac{dI}{dt}$ gives rise to an electromagnetic wave, and as dt gets small, nanoseconds for this experiment, the wave could feasibly turn into an electromagnetic pulse (EMP). If this could be shown, depending on the magnitude of the pulse, a possible application would be damage to electrical components susceptible to EMP.

4. TVR and Pressure Dependence

It was noted that background gas pressures above 50 milli-torr tended to suppress the magnitude of the TVR. Conversely, below this value, a unique *double-spike* phenomenon occurred. At higher pressures, the density of atmospheric neutrals is increased. This corresponds to a decrease in the mean free path between collisions. Consequently, the flux of ions subject to pressure gradients toward the target surface would be reduced, as well as the flux of fast electrons blown off. This would correspond to a reduction in ion concentration around surface whiskers and proportional decreases in electron emission and the magnitude of the TVR. The result is that the voltage response is suppressed. On the other hand, at low pressures, the reduction of the neutral density allows, not only for a higher magnitude response, but also multiple emissions as is indicated by the second spike.

C. CONCLUSIONS

It was concluded that the objectives of the experiment were met. The Target voltage potential was successfully measured, and values ranging from 22 to 140 volts were observed. Subject to the assumption of a few *anomalous free electrons*, and taking into account target surface features, it was claimed that field enhanced emission was the mechanism by which electrons were drawn from the target surface. This was concluded after thermionic electron emission was ruled out due to the low laser energies deposited to the target surface atoms prior to the TVR. Consequently, it could not be claimed that the target was the sole source of the initial electron density as was originally postulated. Interpretation of the TVR, led to the conclusion that an initial electron emission was followed by target surface breakdown and the creation of a dense plasma. Correlation of the TVR with the flash associated with surface breakdown showed that electron emission from the target was the beginning mechanism for plasma creation. These characteristics suggested that what was being observed was the ignition and transition of a LSD wave. Target currents up to 500 amps were calculated suggesting the possibility of electromagnetic pulse phenomena. High pressures tended to suppress the mag-

nitide of the TVR and below 50 milli-torr the TVR showed a double spike indicating multiple emission of electrons from the target surface. In all cases plasmas were formed and damage to the target was primarily due to Unipolar-Arcing.

APPENDIX A

Table 3. RAW DATA: Experimental errors shown in row 1 apply to all subsequent rows.

Resistance (Ohms)	Current (Amps)	Voltage (Volts)	Energy (Joules)
0.1	500.0 ± 0.5	50 ± 5	14.39 ± 0.05
0.3	253.0	76	14.52
0.4	210.0	84	12.58
1.0	25.0	25	14.02
15.0	1.55 ± 0.05	23	14.20
16.0	2.18	35	12.67
20.0	2.05	41	13.65
24.0	0.95	23	13.90
27.0	1.55	42	13.55
33.0	2.10	70	13.90
36.0	1.44	52	13.44
110.0	0.612 ± 0.005	68	13.25
360.0	0.250	90	13.64
430.0	0.233	100	13.85
510.0	0.227	116	13.58
910.0	0.154	140	13.70
1,000,000	$.00009 \pm .000005$	90	14.56
2,000,000	0.000045	90	14.72

APPENDIX B

Table 4. ENERGY PER SHOT

Shot	Energy (J)	Shot	Energy (J)
1	12.24 ± 0.05	14	14.20
2	12.64	15	14.40
3	12.07	16	13.89
4	12.28	17	12.04
5	12.31	18	12.51
6	11.85	19	12.34
7	11.77	20	14.71
8	11.92	21	14.79
9	14.00	22	14.56
10	13.75	23	14.77
11	13.65	24	14.28
12	14.65	25	13.77
13	14.37	Mean energy	13 ± 1

APPENDIX C

Table 5. LASER FLOW, CHARGING CURRENT SETTINGS: These settings were used for every phase of the experiment.

	Pressure (psig)	Flow (scfh)
N_2	10	8
CO_2	10	8
He	8	6
Air	18	4
Charging Voltage	25 KV	

Table 6. OSCILLOSCOPE SETTINGS FOR VOLTAGE MEASUREMENT

Vertical Mode	
Input	50 ohm
Volts Div	As Desired
Polarity	Positive
DC	On
Channel	1
Horizontal Mode	
Trigger	External
Time Div	As Desired
Slope	±
Delay	As desired
Mode	Normal

Table 7. OSCILLOSCOPE SETTINGS FOR TVR CORRELATION, 3 INPUTS

Vertical Mode	
Input (target)	50 ohm
Input (pulse)	1 mega-ohm
Input (flash)	50 ohm
Volts/Div	As Desired
Polarity (target)	Positive
Polarity (pulse)	Negative
Polarity (flash)	Negative
DC	On
Channel (target)	1B
Channel (pulse)	1A
Channel	2B
Horizontal Mode	
Trigger	External
Time Div	As Desired
Slope	±
Delay	As Desired
Mode	Normal

APPENDIX D

This appendix contains the calculation of numbers referred to in the body of the paper. The equations used for the determination of the propagation of experimental errors are listed in Bevington, chapter four [ref. 11].

A. CALCULATION OF TIME TO TVR.

From Figure 22, the laser pulse was extrapolated back to find how far into the laser-target interaction the TVR occurred.

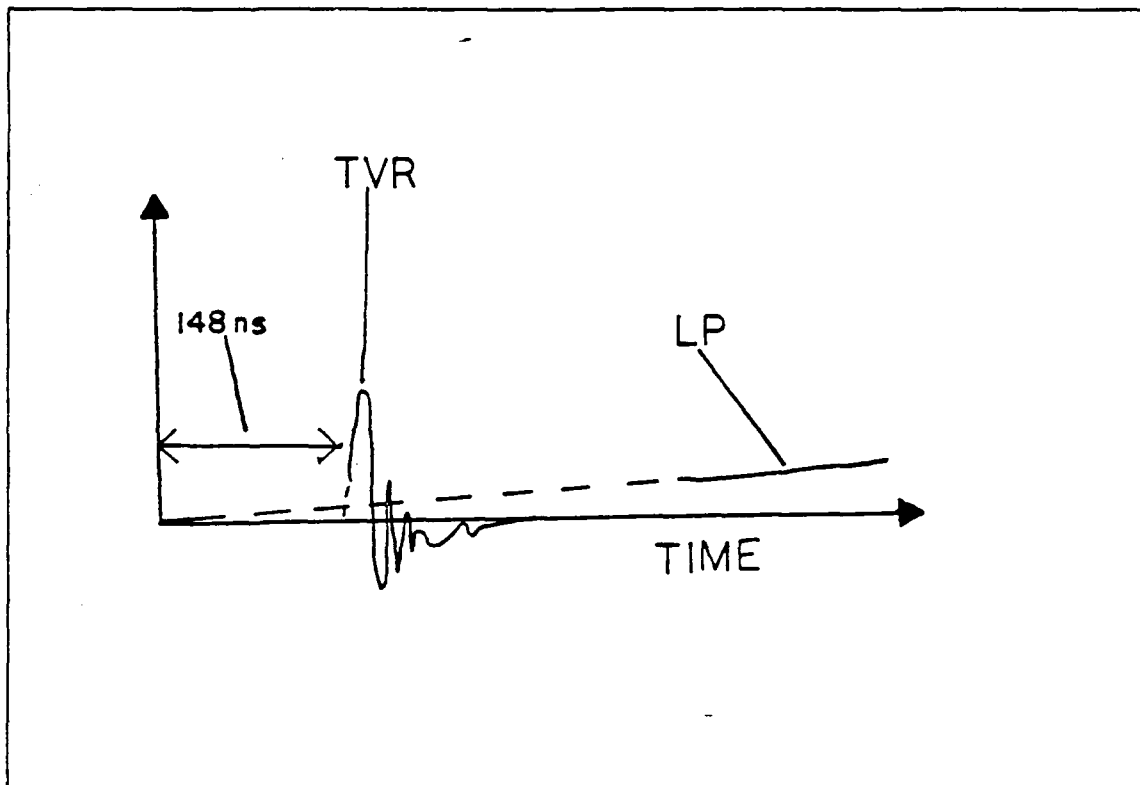


Figure 35. Laser Pulse Extrapolation

Similarly, from Figure 28 the interval was had by inspection. Therefore, averaging these two values, the mean interval to the TVR is reported to be,

$$170 \pm 40 \text{ nanoseconds.}$$

B. CALCULATION OF LASER PULSE INTENSITY

$$\text{Mean Focal Spot Diameter} = 0.35 \pm 0.02 \text{ cm}$$

$$\text{Mean Focal Area} = 0.09 \pm 0.03 \text{ cm}^2$$

$$\text{Mean Energy} = 13 \pm 1 \text{ J}$$

$$\text{Pulse width} = 5 \mu\text{s}$$

$$I = (2.8 \pm 0.6) \times 10^7 \frac{\text{W}}{\text{cm}^2}$$

C. THERMIONIC EMISSION

Graphic integration of the laser pulse from initiation to 170 nanoseconds showed that the energy delivered to the target prior to electron emission was,

$$(1.0 \pm 0.5) \times 10^{-4} \text{ J},$$

or,

$$(6 \pm 3) \times 10^{14} \text{ eV}.$$

For 2024 aluminum the cell structure is face centered cubic (FCC) for which the lattice parameter a_0 is given by,

$$a_0 = \frac{4r}{\sqrt{2}},$$

where,

$$r \equiv \text{Atomic Radius} = 1.82 \text{ \AA}.$$

Therefore the FCC cell surface area is a_0^2 , which equals $7.65 \times 10^{-15} \frac{\text{cm}^2}{\text{cell}}$. Given that there are two atoms per cell surface and the focal spot area is $0.09 \pm 0.03 \text{ cm}^2$, the total number of atoms in the first layer of the focal spot area is given by,

$$N = 6.79 \times 10^{13} \text{ Atoms}.$$

Dividing the total energy delivered to the target in 170 nanoseconds by the total numbers of atoms in the first layer of the focal spot area gives,

$$9 \pm 4 \frac{\text{eV}}{\text{atom}} .$$

D. CALCULATION OF MEAN TVR PULSE WIDTH

The seven pulse widths from **Table 1** on page 23 were averaged. Therefore the mean pulse width of the TVR is reported to be,

$$30 \pm 9ns.$$

LIST OF REFERENCES

1. Schwirzke, F., **Unipolar Arcing, a Basic Damage Mechanism**, National Bureau of Standards Special Publication 669, Laser Induced Damage in Optical Materials, pp 458-478, United States Department of Commerce, 1982.
2. Robson, A.E., and Thonemann, P.C., **An Arc Maintained on an Isolated Metal Plate Exposed to Plasma**, Proceedings of the Physical Society of London. Volume 73, pp 508-512, March 1959.
3. Schwirzke, F., **Plasma Jets Emitted by Unipolar Arcing from Spherical Targets**, Laser Interaction and Related Plasma Phenomena, Volume 7, Plenum Publishing Corporation, 1986.
4. Harrison, D.E., **Laser Effects Handbook 3 Laser Absorption Wave Phenomena**, Naval Postgraduate School report NPS-61NB-75121, Edited by J.R. Neighbours, December 1975.
5. Walters, C.T., **Proceedings of the 1973 DOD Laser Effects/Hardening Conference**, Volume V., Edited by Norman F. Harmon, pp. 197-202, June 1974.
6. Wojtowich, A.R., **Background Gas Pressure Dependence of Unipolar Arcing on Soda Lime Glass and Plastic Induced by a CO₂ Pulsed Laser**, Master's Thesis, Naval Postgraduate School, Monterey, California, June 1988.
7. Chen, F.F., **Introduction to Plasma Physics and Controlled Fusion**, second edition, Volume 1, Plenum Press, 1984.
8. Weston, R.C., **CO₂ Pulsed Laser Damage Mechanisms and Assessments of Plasma Effects (Focused Beam)**, Master's Thesis, Naval Postgraduate School, Monterey, California, December 1986.

9. Hall, R.B., Maher, W.E., and P.S. Wei, **An Investigation of Laser Supported Detonation Waves**, AFWL-TR-73-28, Boeing Aerospace Company, Seattle, Washington, pp 4-32, 120-146, June 1972.
10. Schriempf, J.T., **Response of Materials to Laser Radiation: a Short Course**, NRL Report 7728, Naval Research Laboratory, Washington, D.C., July 10, 1974.
11. Bevington, P.R., **Data Reduction and Error Analysis for the Physical Sciences**, McGraw-Hill Book Company, New York, 1969.

INITIAL DISTRIBUTION LIST

	No. Copies
1. Defense Technical Information Center Cameron Station Alexandria, VA 22304-6145	2
2. Library, Code 0142 Naval Postgraduate School Monterey, CA 93943-5002	2
3. Office of Naval Research Attn: Dr. R. Pohanka 800 N Quincy Street Arlington, VA 22217	1
4. Naval Research Laboratory Attn: Dr. T. Wieting Washington, DC 20375	1
5. Professor F. R. Schwirzke, Code 61Sw Department of Physics Naval Postgraduate School Monterey, CA 93943-5000	3
6. Professor A. W. Cooper, Code 61Cr Department of Physics Naval Postgraduate School Monterey, CA 93943-5000	1
7. Lieutenant Richard Harkins Surface Warfare Officers School Command New Port, RI 02841-5012	2